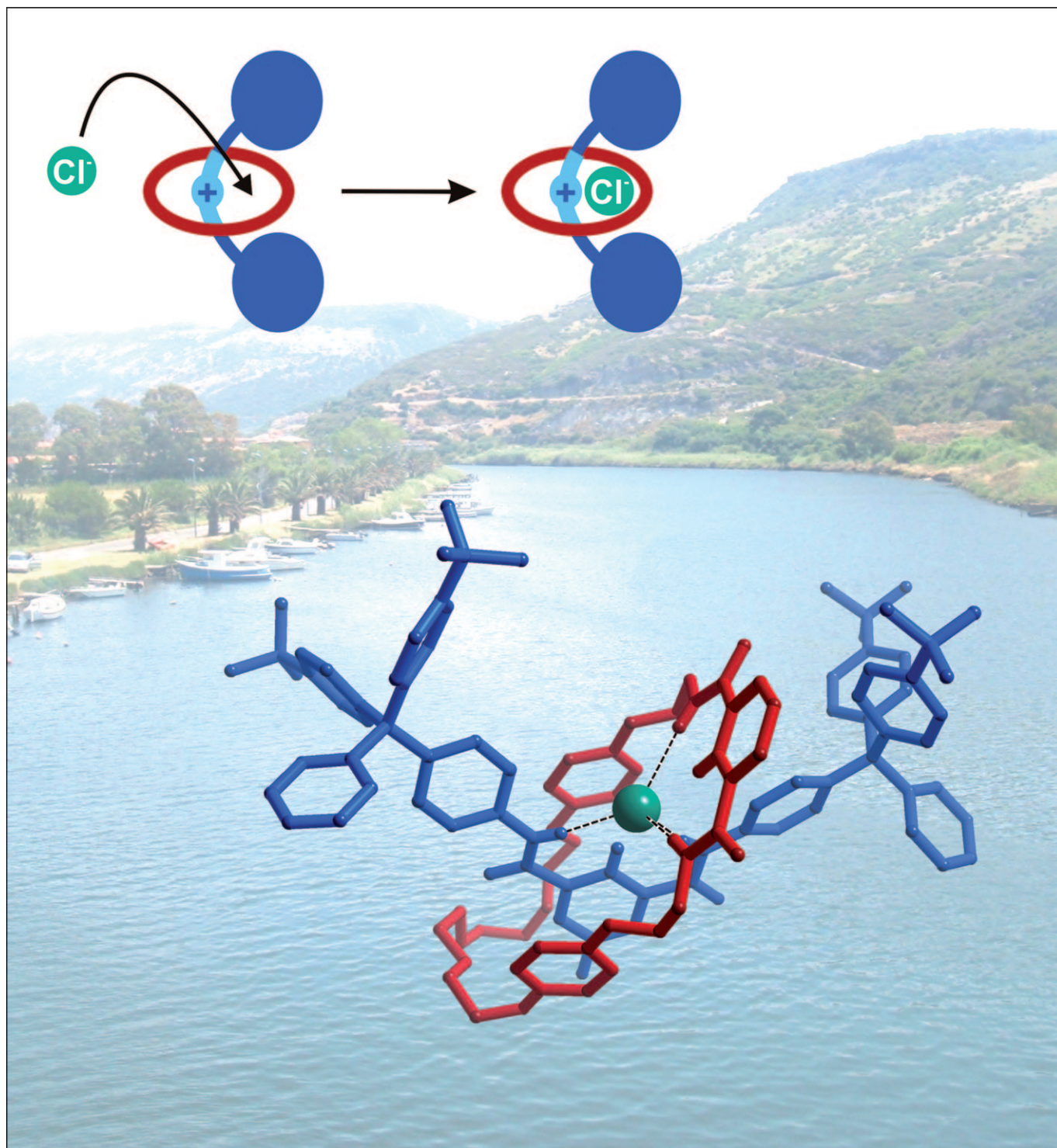


## Rotaxanes Capable of Recognising Chloride in Aqueous Media

Laura M. Hancock,<sup>[a]</sup> Lydia C. Gilday,<sup>[a]</sup> Sílvia Carvalho,<sup>[b]</sup> Paulo J. Costa,<sup>[b]</sup> Vítor Félix,<sup>[b]</sup>  
Christopher J. Serpell,<sup>[a]</sup> Nathan L. Kilah,<sup>[a]</sup> and Paul D. Beer<sup>\*[a]</sup>



**Abstract:** A new, versatile chloride-anion-templating synthetic pathway is exploited for the preparation of a series of eight new [2]rotaxane host molecules, including the first sulfonamide interlocked system.  $^1\text{H}$  NMR spectroscopic titration investigations demonstrate the rotaxanes' capability to selectively recognise the chloride anion in competitive aqueous solvent

media. The interlocked host's halide binding affinity can be further enhanced and tuned through the attachment of electron-withdrawing substituents and by increasing its positive

**Keywords:** anions • molecular recognition • rotaxanes • supramolecular chemistry • template synthesis

charge. A dicationic rotaxane selectively binds chloride in 35 % water, where-in no evidence of oxoanion binding is observed. NMR spectroscopy, X-ray structural analysis and computational molecular dynamics simulations are used to account for rotaxane formation yields, anion binding strengths and selectivity trends.

## Introduction

Motivated by the fundamental roles negatively charged species play in a range of chemical, biological, medical and environmental processes, the field of anion supramolecular chemistry has expanded enormously during the past few decades.<sup>[1]</sup> In spite of the numerous synthetic acyclic and macrocyclic receptors reported to date, the degree of selectivity exhibited by biological anion-binding proteins far exceeds any synthetic receptor. Nature's strong and highly selective binding of sulfate<sup>[2]</sup> and phosphate<sup>[3]</sup> anions in water, for example, is achieved by an intricate network of hydrogen bonds buried deep inside specific proteins and not on the surface exposed to the solvent. This suggests that, to significantly "raise the bar" in the level of anion binding strength and selectivity exhibited by current synthetic receptors, the design and synthesis of much more elaborate three dimensional receptor systems is required, in which the binding site is in a protected hydrophobic microenvironment that enables the total encapsulation of the anionic guest species. Taking this into account, we surmised that the construction of such sophisticated target receptors would require unprecedented, innovative, anion-template synthetic methodologies.

Although various serendipitous discoveries in which anions have been shown to control the assembly of poly-metallic cluster and cage complexes abound in the literature,<sup>[4]</sup> the strategic use of anions as potential templating reagents for the assembly of designed molecular architectures remains very much in its infancy.<sup>[5]</sup> Importantly, this may be a consequence of their perceived diffuse nature (small

charge/radius ratio) and weakly pronounced coordination preferences (no ligand field effects). Hydrogen bonds formed with anions are weaker and more difficult to control as compared with metal–cation coordinative bonds. Rare examples in which specific inorganic anions have been demonstrated to play a templating role in the synthesis of organic-based systems have been largely restricted to expanded porphyrins<sup>[6]</sup> and polypyrrolic,<sup>[7]</sup> hexaurea<sup>[8]</sup> and peptidic<sup>[9]</sup> macrocycles.

In spite of the huge interest currently being shown in the construction of mechanically bonded molecules for nanotechnological applications as molecular switches and machines,<sup>[10]</sup> the potential of their unique topological cavities in host–guest chemistry has been largely neglected.<sup>[11]</sup> This is especially the case for the recognition of anions.<sup>[12]</sup> We have previously exploited the chloride anion in the templated synthesis of rotaxane and catenane systems through Grubbs'-catalysed ring-closing metathesis (RCM) reactions.<sup>[13]</sup>


We have discovered, however, that the RCM catalyst is unsuitable when the axle or macrocycle precursor components contain competing ligating functional groups, such as a pyridyl group. To overcome this problem, we recently reported an alternative synthetic route for the preparation of a new [2]rotaxane, containing a pyridyl macrocyclic wheel.<sup>[14]</sup> The synthetic versatility of this new route is illustrated herein by the preparation of a series of eight new [2]rotaxanes, including the first sulfonamide interlocked system, the three-dimensional interlocked-binding-domain cavities of which can be tuned to exhibit high degrees of chloride anion selectivity in competitive aqueous solvent mixtures.<sup>[15]</sup> In addition, NMR spectroscopic and X-ray structural investigations, in combination with computational molecular dynamics simulations, are used to rationalise the observed rotaxane formation yields, anion binding affinities and selectivity trends.

## Results and Discussion

In a preliminary report, we described the preparation of a rotaxane through a new synthetic pathway.<sup>[14]</sup> By varying the nature of the condensation reactants and reaction condi-

[a] L. M. Hancock, L. C. Gilday, C. J. Serpell, Dr. N. L. Kilah, Prof. P. D. Beer  
Chemistry Research Laboratory, Department of Chemistry  
University of Oxford, Mansfield Road, Oxford, OX1 3TA (UK)  
Fax: (+44) 186-527-2690  
E-mail: paul.beer@chem.ox.ac.uk

[b] Dr. S. Carvalho, Dr. P. J. Costa, Prof. V. Félix  
Departamento de Química  
CICECO and Secção Autónoma de Ciências da Saúde  
Universidade de Aveiro, 3810-193 Aveiro (Portugal)

 Supporting information for this article is available on the WWW under <http://dx.doi.org/10.1002/chem.201002076>.

tions, the synthetic versatility of this new rotaxation method was investigated, with the production of eight new rotaxane host systems, the orthogonal interlocked-cavity dimensions, electronic substituents, degree of positive charge and macrocycle-ring cavity size of which significantly influence the degree of selective chloride anion binding affinity in competitive aqueous solvent media.

**Synthesis of rotaxanes:** It was discovered that the yield of the original rotaxane could be significantly improved upon, in fact nearly doubled, by limiting the amount of triethylamine used in the reaction mixture. Thus, in a modified procedure, the reaction of bis(amine) **2** (as opposed to the hydrogen chloride salt)<sup>[16]</sup> with 3,5-bis(chlorocarbonyl)pyridine in the presence of a pyridinium axle component **1-Cl**<sup>[13a]</sup> in dry CH<sub>2</sub>Cl<sub>2</sub> and triethylamine (2.5 equiv) produced rotaxane **5-Cl** in an improved isolated yield of 56% (Scheme 1).

Since the pyridinium motif is susceptible to reacting with nucleophiles,<sup>[17]</sup> we postulated that excess triethylamine in the reaction mixture may lead to degradation of the pyridinium axle component. Exploiting this modified synthetic methodology, a range of new [2]rotaxanes were prepared

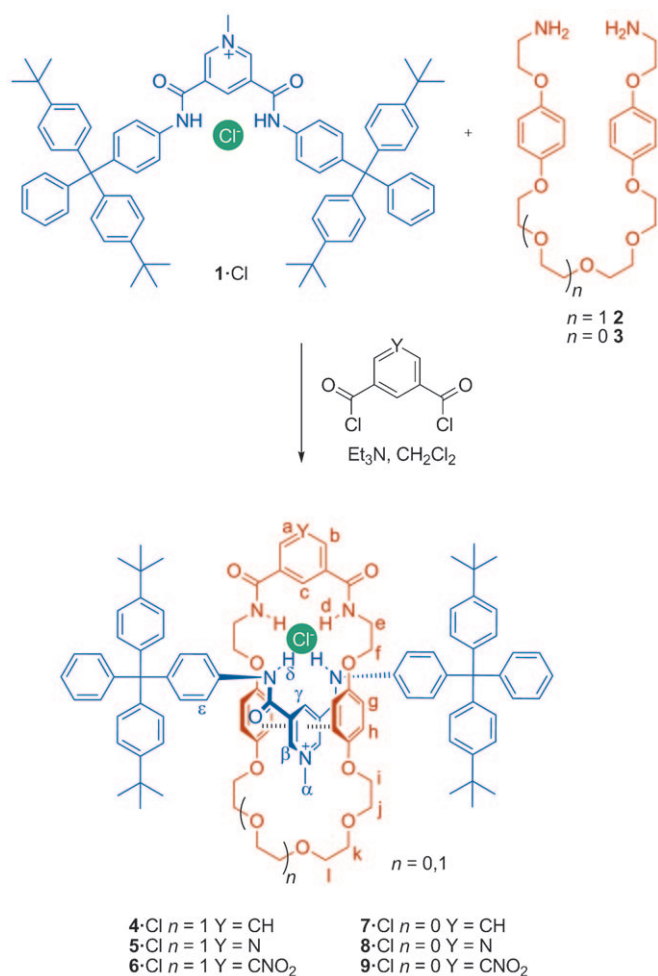
through the addition of an appropriate bis(acid chloride) to a mixture of axle **1-Cl** and either the four or five oxygen polyether-containing bis(amine) in dichloromethane in the presence of triethylamine (Scheme 1). After preparative TLC purification the rotaxanes were isolated in 36–60% yields (Table 1). The lower yields of the rotaxanes contain-

Table 1. Yields of [2]rotaxanes by using the modified synthetic route.

	4-Cl	5-Cl	6-Cl	7-Cl	8-Cl	9-Cl
Yield [%]	60	56	55	42	36	41

ing the shorter polyether chain are attributed to unfavourable steric interactions between the methyl group of the pyridinium unit and the macrocyclic component, which is corroborated by computational molecular dynamics simulations (vide infra).

The <sup>1</sup>H NMR spectrum of rotaxane **4-Cl**, along with those of its component macrocycle<sup>[18]</sup> and axle **1-Cl** for comparison, is shown in Figure 1. [2]Rotaxane **4-Cl** displays consid-



Scheme 1. Synthesis of [2]rotaxanes (**4–9**)-Cl.

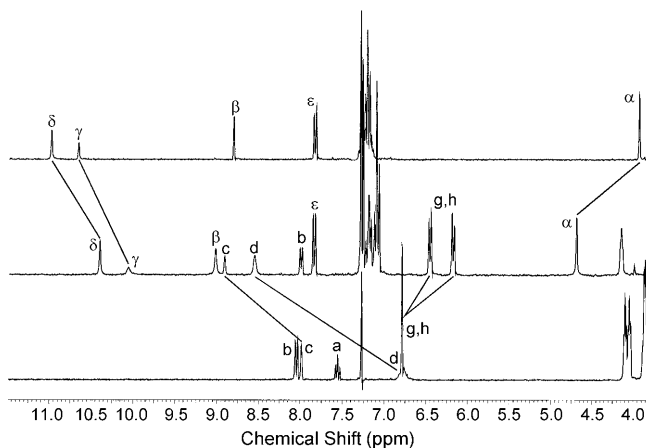


Figure 1. <sup>1</sup>H NMR spectra in CDCl<sub>3</sub> at 293 K of axle **1-Cl** (top), [2]rotaxane **4-Cl** (middle) and component macrocycle (bottom).

erable upfield shifts of the amide ( $\delta$ ) and para-pyridinium ( $\gamma$ ) protons, corresponding to polarisation of the chloride anion away from the binding cleft as a result of halide anion recognition by the macrocycle's isophthalamide cavity. This is further signified by downfield shifts of the amide ( $d$ ) and cavity isophthalamide ( $c$ ) protons as they become deshielded by the halide's negative charge. The proton signals associated with the hydroquinone environments ( $g$  and  $h$ ) of the macrocycle have moved upfield and split appreciably, which is characteristic of  $\pi$ – $\pi$  donor–acceptor interactions between the electron-rich hydroquinones and the positively charged, electron-deficient pyridinium motif. Finally, the signal corresponding to the methyl protons ( $\alpha$ ) of the pyridinium axle has moved significantly upfield, which is indicative of hydrogen bonding between these protons and the oxygen atoms of the macrocycle's polyether chain.



Further characterisation of the structure of [2]rotaxane **4**·Cl was obtained by 2D  $^1\text{H}$ - $^1\text{H}$  ROESY spectroscopy (Figure 2). The  $^1\text{H}$  NMR ROESY spectrum displays a

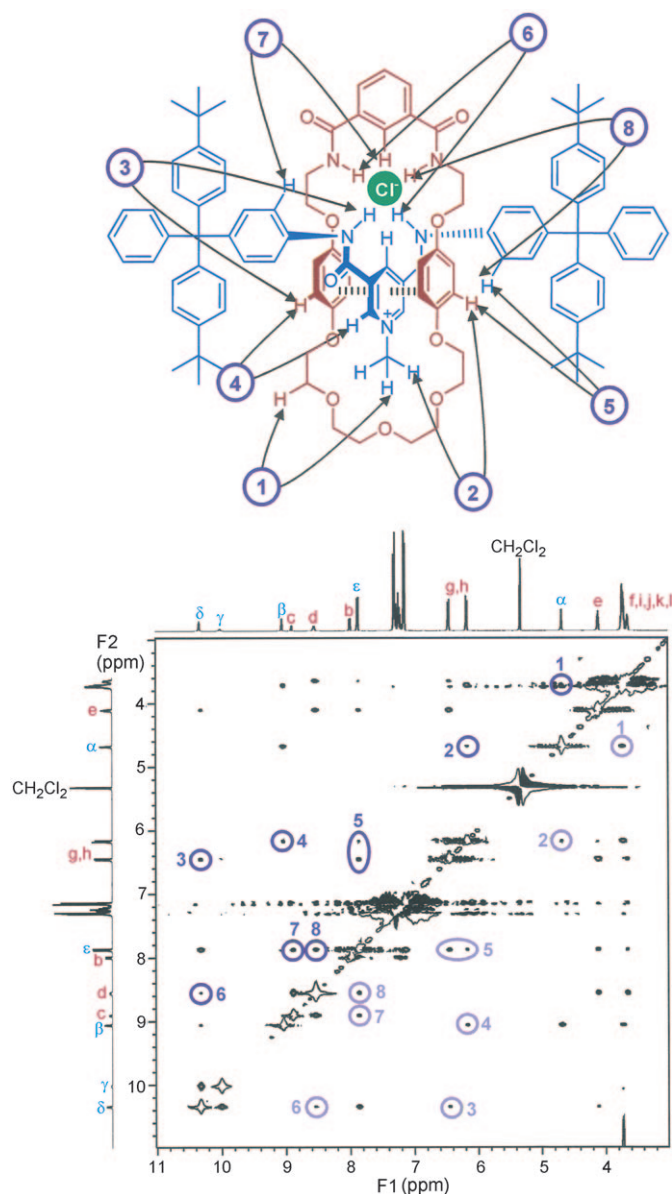
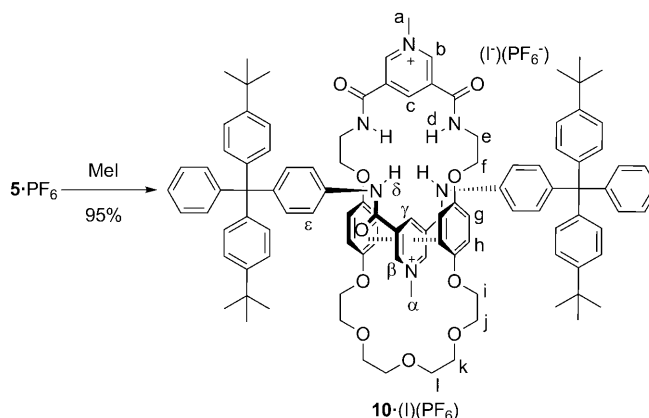


Figure 2.  $^1\text{H}$ - $^1\text{H}$  ROESY spectrum of [2]rotaxane **4**·Cl in  $\text{CD}_2\text{Cl}_2$  at 293 K. Cross-couplings are shown on the schematic diagram.

number of through-space correlations between the two separate components of the [2]rotaxane. Important interactions include 4 ( $\beta \rightarrow \text{g,h}$ ) and 3 ( $\delta \rightarrow \text{g,h}$ ), which are characteristic of  $\pi$ - $\pi$  stacking between the protons of the electron-rich hydroquinone unit and the electron-deficient pyridinium unit, suggesting that the axle component is threaded through the centre of the macrocycle. Interaction 6 ( $\delta \rightarrow \text{d}$ ) confirms the cavity amide protons are in close proximity to each other as they converge into the binding domain to complex chloride.

NOEs 5 ( $\epsilon \rightarrow \text{g,h}$ ), 7 ( $\epsilon \rightarrow \text{c}$ ) and 8 ( $\epsilon \rightarrow \text{d}$ ) indicate that the axle stoppers are spatially close to both the macrocycle cavity and the hydroquinone protons, confirming that the axle resides in the macrocycle in the depicted orientation. Finally, interactions 1 ( $\alpha \rightarrow \text{f,i-l}$ ) and 2 ( $\alpha \rightarrow \text{g,h}$ ) reveal that the pyridinium methyl protons are in close proximity to both the polyether chain of the macrocycle (through hydrogen-bonding interactions previously described) and also to the hydroquinone protons.

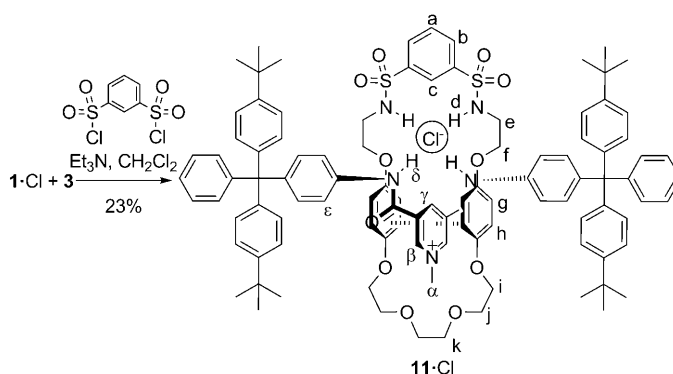
To investigate the effect of increased charge on the anion-recognition properties of this class of rotaxane host systems, a novel dicationic [2]rotaxane **10**·(I)( $\text{PF}_6$ ) was synthesised. Rotaxane **5**·Cl was converted to the hexafluorophosphate salt before reacting with MeI to give **10**·(I)( $\text{PF}_6$ ) (Scheme 2).



Scheme 2. Synthesis of dicationic [2]rotaxane **10**·(I)( $\text{PF}_6$ ).

It was also possible to synthesise the first sulfonamide containing rotaxane **11**·Cl by using this methodology (Scheme 3). The yield of the formation of this rotaxane was lower than those depicted in Scheme 1, which suggests chloride anion templation is not as efficient with the sulfonamide motif.

However, it is notable that analogous rotaxanation reactions with phthaloyl and terephthaloyl acid chlorides failed to produce any evidence of rotaxane formation. These ob-

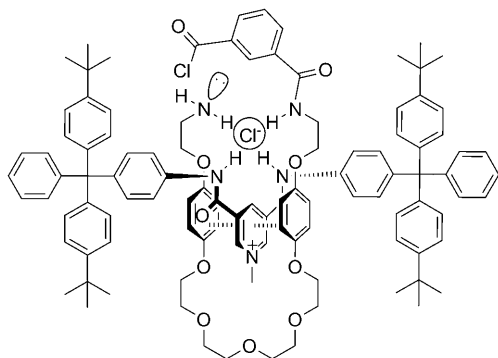


Scheme 3. Synthesis of sulfonamide-containing [2]rotaxane **11**·Cl.

servations highlight the importance of the isophthalamide chloride anion recognition motif in mechanical bond formation.

**Investigations into the role of the templating anion:** We carried out a series of experiments in order to gain insight into the mechanism of this rotaxation reaction and establish the importance of the anion in templating the formation of the interlocked species.

From comparison of the  $^1\text{H}$  NMR spectrum of an equimolar mixture of axle component **1**·Cl and bis(amine) precursor **2** with the spectra of the separate compounds (all in  $\text{CDCl}_3$ ), no evidence of  $\pi$ - $\pi$  stacking interactions between the axle pyridinium motif and the hydroquinone units of **2** was observed. This suggests that the rotaxation reaction proceeds via an intermediate assembly of components (Scheme 4), in which an amine has reacted with one acid

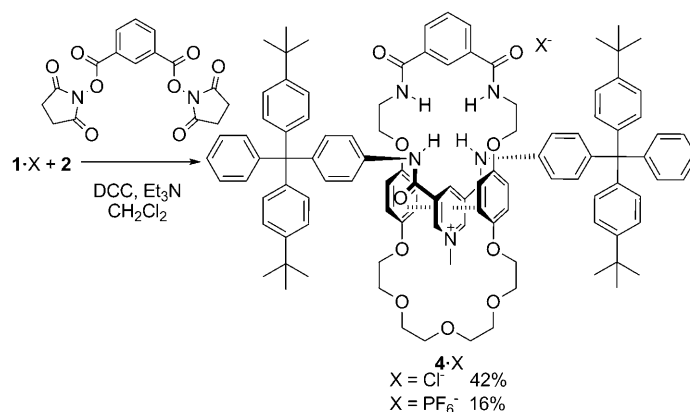


Scheme 4. Proposed rotaxane intermediate.

chloride group and the chloride anion, through hydrogen bonding, templates the intramolecular amide ring-closing condensation reaction around the pyridinium axle component to afford the interlocked product. This postulation places great importance on the templating role of the halide anion and so it was important to repeat the reaction in the absence of chloride.

The condensation reaction was carried out by using an activated ester, which was synthesised by reacting isophthalic acid with *N*-hydroxysuccinamide in the presence of the coupling reagent *N,N*-dicyclohexylcarbodiimide (DCC; Scheme 5). The reaction was carried out both with the chloride salt and with the hexafluorophosphate salt of the pyridinium axle component. In the presence of the chloride anion the yield of the rotaxation reaction was 42 %, whereas the rotaxane was obtained in only 16 % yield when **1**·PF<sub>6</sub> was used. Thus, the presence of chloride as a templating reagent significantly enhances the yield of the rotaxane production.<sup>[19]</sup>

**X-ray crystal structures of rotaxanes:** Crystals suitable for X-ray diffraction were prepared for rotaxanes **4**·Cl and **9**·Cl by gaseous diffusion of diisopropyl into solutions of the ro-



Scheme 5. Synthesis of [2]rotaxane **4** by using DCC coupling.

taxanes in dichloromethane and benzene, respectively. Data collection was undertaken at beamline I19 of Diamond Light Source.

The structures (Figure 3) confirm the interlocked nature of the respective systems and the location of the chloride anion in the expected binding site, encapsulated by the orthogonal hydrogen-bonding array. The distance between the chloride anion and the centre of the binding pocket ( $N_{\text{mass}}$ ) defined by the four nitrogen atoms of the N-H binding sites (two amide nitrogen atoms of the pyridinium axle and two

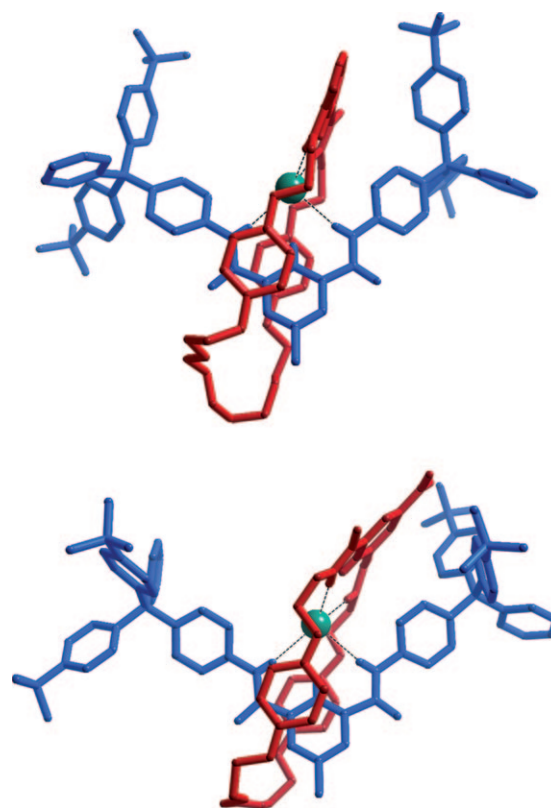


Figure 3. X-ray crystal structures of **4**·Cl (top) and **9**·Cl (bottom). Disorder and non-protic hydrogen atoms were omitted for clarity.

amide nitrogen atoms of the macrocycle) was calculated to be  $0.567 \pm 0.001$  Å for **4**-Cl and  $0.649 \pm 0.003$  Å for **9**-Cl, suggesting that the binding pocket of **4** is more favourably disposed to chloride inclusion.

The effect of the longer polyether chain in **4**-Cl, as opposed to **9**-Cl, is also apparent. Whereas in **4**-Cl the polyether chain appears to have the capacity to swing back and forth over the pyridinium methyl group with ease, it is less clear that **9**-Cl possesses the necessary degrees of freedom for this process to occur readily. The interactions between the polyether and the pyridinium methyl as expressed in the polyether chain length are critical to synthesis (as demonstrated above) and anion binding (vide infra). The greater conformational flexibility in **4**-Cl may allow an induced-fit mechanism to operate more successfully.<sup>[20]</sup>

**Rotaxane anion binding properties:** To study the anion-binding properties of the rotaxanes, it was necessary to exchange the chloride templating anion for the non-coordinating hexafluorophosphate anion. This was achieved in quantitative yield by washing a solution of the rotaxane in  $\text{CHCl}_3$  with an  $\text{NH}_4\text{PF}_6(\text{aq})$  solution. Anion exchange of these [2]rotaxanes was observed, by  $^1\text{H}$  NMR spectroscopy, to have only a small effect on the position of the cationic pyridinium axle component within the macrocycle. Indeed, 2D ROESY spectroscopic evidence (see the Supporting Information) indicates that the structure remains interlocked with the same coupling interactions between proximal protons observed as were present in the 2D ROESY spectrum of the chloride salt of the same rotaxane. The only significant differences between the chloride and hexafluorophosphate salts of the [2]rotaxanes are that the signals corresponding to the cavity protons in which the chloride resided are observed to move upfield when the templating anion is removed.

The anion-binding properties of rotaxanes (**4**–**9**)- $\text{PF}_6$  were investigated initially by  $^1\text{H}$  NMR titration experiments with TBA salts of  $\text{Cl}^-$ ,  $\text{H}_2\text{PO}_4^-$  and  $\text{OAc}^-$  in 1:1  $\text{CDCl}_3/\text{CD}_3\text{OD}$ . It was possible to monitor the chemical shift perturbations of cavity protons  $\epsilon$  and  $\gamma$ , and *ortho*-pyridinium proton  $\beta$  as a function of the concentration of the anion. However, winEQNMR2<sup>[21]</sup> was unable to determine the association constant values for chloride binding in this solvent system as the halide is bound extremely strongly ( $K > 10^4 \text{ M}^{-1}$ ). In stark contrast to this, the axle **1**- $\text{PF}_6$  only weakly binds chloride in this solvent system ( $K = 125 \text{ M}^{-1}$ ), and exhibits a pronounced selectivity preference for the basic dihydrogen phosphate and acetate anions.<sup>[13a]</sup> Interestingly, the novel sulfonamide-containing [2]rotaxane **11**- $\text{PF}_6$  proved to bind chloride relatively weakly, exhibiting an association constant of  $1500 \text{ M}^{-1}$ , which correlates with the rotaxane's lower yield and indicates that the halide anion is a less efficient templating reagent for this type of compound. Moreover, computational molecular dynamics simulations support this conjecture (vide infra).

Analogous anion-binding titrations were undertaken in the presence of 10% water, and winEQNMR2 was used to calculate the association constants, which are reported in

Table 2. The monocationic rotaxanes were observed to bind chloride strongly even in this competitive aqueous solvent mixture, whereas the oxoanions were complexed only

Table 2. Association constants,  $K$  [ $\text{M}^{-1}$ ], of [2]rotaxanes with  $\text{Cl}^-$ ,  $\text{H}_2\text{PO}_4^-$  and  $\text{OAc}^-$  in 45:45:10  $\text{CDCl}_3/\text{CD}_3\text{OD}/\text{D}_2\text{O}$  at 293 K.<sup>[a]</sup>

	$\text{Cl}^-$	$\text{H}_2\text{PO}_4^-$	$\text{OAc}^-$
<b>4</b> - $\text{PF}_6$	1190	120	180
<b>5</b> - $\text{PF}_6$	1500	60	110
<b>6</b> - $\text{PF}_6$	1800	170	180
<b>7</b> - $\text{PF}_6$	860	110	120
<b>8</b> - $\text{PF}_6$	1450 <sup>[b]</sup>	120	250
<b>9</b> - $\text{PF}_6$	1175	150	200

[a] Obtained by monitoring proton  $\beta$ . Error < 10%. [b] Error < 15%.

weakly, despite the greater basicity of these anions. These results indicate that the respective interlocked binding pockets are of complementary size to chloride and the pseudo-tetrahedral binding environment created by the convergent amide groups is able to satisfy the coordination sphere of the spherical chloride anion.<sup>[22]</sup> Furthermore, whilst addition of chloride to the [2]rotaxanes produces downfield shifts in cavity pyridinium proton  $\gamma$ , addition of either dihydrogen phosphate or acetate anions causes an upfield perturbation of this proton signal, presumably as a consequence of a conformational change in the [2]rotaxane, since these anions are too large to penetrate the interlocked binding cavity and, consequently, associate externally.

Of the monocationic rotaxanes, those with the larger macrocyclic component were observed to complex chloride significantly more strongly, which contrasts with what might be predicted on the grounds of preorganisation. This may be attributed to the binding of chloride causing unfavourable steric interactions between the pyridinium methyl group of the axle and the polyether chain of the smaller macrocycle, which is suggested in the solid-state structure of **4**-Cl (Figure 3) and further rationalised in molecular dynamics simulations (vide infra).

As expected, the rotaxanes containing the electron-withdrawing pyridine functionalities, **5**- $\text{PF}_6$  and nitro-isophthalamide **6**- $\text{PF}_6$ , display an enhanced affinity for chloride. This is a consequence of the increased acidity of the amide protons and, thus, their hydrogen-bonding ability to the anion in question.

As an extension of this concept, the novel dicationic [2]rotaxane **10**-( $\text{PF}_6$ )<sub>2</sub> was shown to bind chloride with an association constant of  $3000 \text{ M}^{-1}$  in the 10% water solvent system. This high association constant is attributed to a combination of increased charge electrostatics and, thus, increased acidity of the cavity protons of the rotaxane. Consequently, anion-binding studies were carried out in a solvent system containing a higher percentage of water. The limiting factor of these studies was the solubility of the rotaxane, which contains large lipophilic stopper groups. Therefore, the anion properties of rotaxane **10**-( $\text{PF}_6$ )<sub>2</sub> were investigated in 65:35 [ $\text{D}_6$ ]acetone/ $\text{D}_2\text{O}$ , and the results are given in Table 3.

Table 3. Association constants,  $K$  [ $\text{M}^{-1}$ ], of [2]rotaxane **10**·(PF)<sub>2</sub> with Cl<sup>−</sup>, H<sub>2</sub>PO<sub>4</sub><sup>−</sup> and OAc<sup>−</sup> in 65:35 [D<sub>6</sub>]acetone/D<sub>2</sub>O at 293 K.<sup>[a]</sup>

	Cl <sup>−</sup>	H <sub>2</sub> PO <sub>4</sub> <sup>−</sup>	OAc <sup>−</sup>
<b>10</b> ·(PF) <sub>2</sub>	500	NB	NB

[a] Obtained by monitoring proton  $\gamma$ . Error < 10%. NB denotes no binding.

Remarkably, chloride is still bound with considerable strength in 35 % water, whereas no binding of oxoanions is observed. This rotaxane displays total selectivity for chloride over the more basic dihydrogen phosphate and acetate in this solvent mixture, which is again attributable to the complementary size and shape of chloride for the rotaxane's binding cavity.

**Molecular dynamics simulations:** Further insights into the formation and anion binding properties of representative rotaxanes **4**, **7** and **11** were investigated by means of molecular mechanics (MM) and molecular dynamics (MD) simulations, by using Amber10 software<sup>[23]</sup> with the general Amber force field (GAFF)<sup>[24]</sup> parameters (see Supporting Information).

Since the X-ray crystal structures of **4**·Cl and **9**·Cl reveal that chloride is bound in a *syn-syn* co-conformation (Figure 3), suitable *syn-syn* low energy co-conformations for the rotaxane associations **4**·Cl, **4**·OAc, **4**·H<sub>2</sub>PO<sub>4</sub>, **7**·Cl, **7**·OAc, **7**·H<sub>2</sub>PO<sub>4</sub> and **11**·Cl were generated in the gas phase through the quenched MD approach, as described in detail in the Supporting Information. These co-conformations were then immersed in an equilibrated cubic-box solvent mixture of CHCl<sub>3</sub>/CH<sub>3</sub>OH/H<sub>2</sub>O (45:45:10) and subjected to classical MD simulations for 10 ns.

We start by discussing chloride-templated rotaxane formation and their stability by analysing the MD simulations for **4**·Cl, **7**·Cl and **11**·Cl. Snapshots of representative binding arrangements taken from these MD simulations are shown in Figure 4. In all three cases, the main structural features of the respective binding arrangements found in the gas phase are retained in solution over the entire time of the MD simulations and are consistent with the pseudo-tetrahedral binding arrangement found in the single-crystal X-ray structure of **4**·Cl, in which the chloride anion is bound to the macrocycle and the pyridinium axle by four N–H···Cl<sup>−</sup> hydrogen bonds. Furthermore, the axle's pyridinium ring is almost parallel to the two hydroquinone entities, stabilised by  $\pi$ – $\pi$  interactions.

For **4**·Cl and **7**·Cl associations, the  $N_{\text{mass}} \cdots \text{Cl}^-$  average distances are quite short (1.360 and 1.424 Å, respectively) with small standard deviations, which indicates that, in both cases, the chloride anion fits well inside the binding pocket, tightly hydrogen bonded to the four N–H binding sites. In contrast, for **11**·Cl the average  $N_{\text{mass}} \cdots \text{Cl}^-$  distance increases to 3.391 Å with a very large standard deviation of 2.08 Å, which suggests that the orthogonal assembly between the axle and the macrocycle with a sulfonamide motif is not very stable. In fact, the chloride interlocked rotaxane ar-

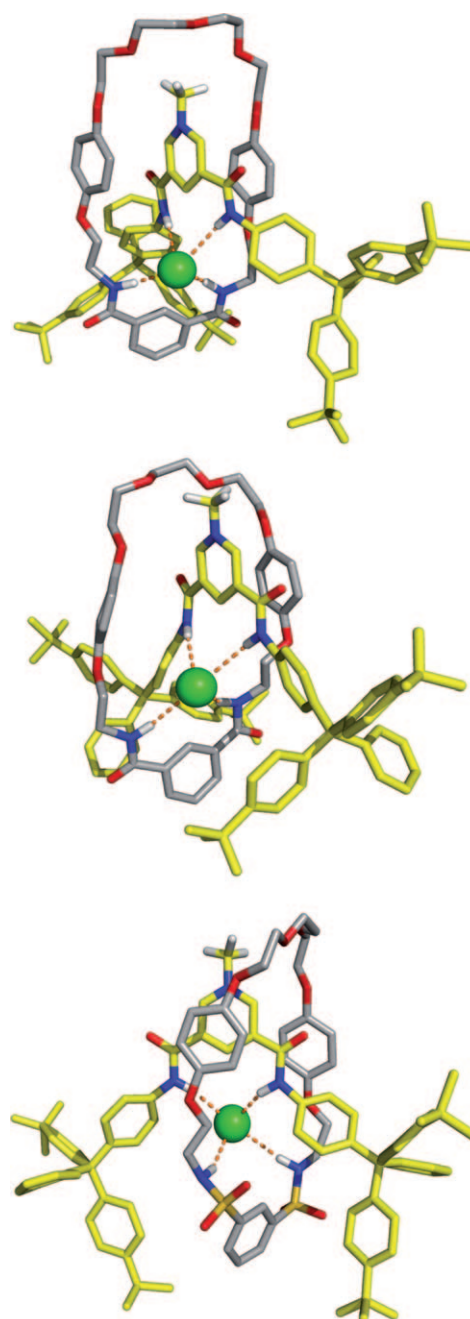


Figure 4. Snapshots of **4**·Cl (top), **7**·Cl (middle) and **11**·Cl (bottom) taken at 5 ns of MD simulation. Carbon atoms of the macrocycle and pyridinium axle are shown in grey and yellow, respectively. Hydrogen bonds are represented as orange dashed lines. For clarity, only the N-methyl and N–H hydrogen atoms are shown.

angement is interrupted after 8.5 ns of the MD simulation, leading to the large standard deviation reported. These structural trends are also evident from comparison of the probability density function (PDF) of the  $N_{\text{mass}} \cdots \text{X}^-$  distances for the three rotaxanes, presented in the Supporting Information. Indeed, for **4**·Cl and **7**·Cl, sharp distributions centred on the  $N_{\text{mass}} \cdots \text{X}^-$  average distances are obtained, while for **11**·Cl the distribution is significantly more diffuse. The  $N_{\text{mass}} \cdots \text{X}^-$  average distances and their standard deviations, as



well as the PDFs, correlate very well with the experimentally observed rotaxane formation yields and chloride binding affinities, which follow the order  $4\text{-Cl} > 7\text{-Cl} > 11\text{-Cl}$  (see above). The relatively more stable chloride structural arrangement of  $4\text{-Cl}$ , when compared to  $7\text{-Cl}$ , correlates with smaller average distances and standard deviations (with sharper PDFs) and a larger observed yield. These results are also consistent with the smaller yield of sulfonamide rotaxane  $11\text{-Cl}$  that is indicative of less efficient chloride anion templation, which can be caused by the different conformational restrictions imposed by the macrocycle's  $\text{R-SO}_2\text{-R}$  tetrahedral fragment on the  $\text{N-H}$  bond directionality. This can be seen in Figure 4 (bottom), in which the two  $\text{N-H}$  binding groups from the macrocycle are clearly out of the plane of the sulfonamide "head", whilst in the isophthalamide counterparts (top and middle), they are almost in the plane.

It was suggested earlier that the difference between the yields of formation of  $4\text{-Cl}$  and  $7\text{-Cl}$  is attributable to the unfavourable steric interactions between the methyl group of the pyridinium axle and the polyether chains of the macrocycle. This observation is corroborated by the MD simulations. Figure 5 depicts the grid contours representing the his-

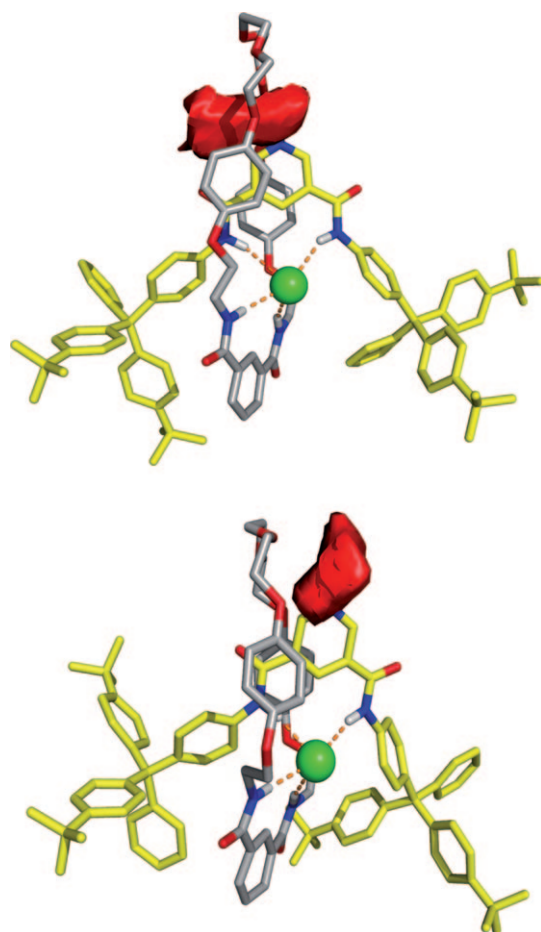


Figure 5. Grid representation (red) of the histograms for the location of the methyl carbon atom in the pyridinium axle (yellow) over the 10 ns simulation of  $4\text{-Cl}$  (top) and  $7\text{-Cl}$  (bottom). A density contour value of 10 was used.

togram built with the spatial positions occupied by the  $N$ -methyl carbon atom of the pyridinium over the entire simulation time for both rotaxanes. It is clear that the density of the methyl carbon atom in  $4\text{-Cl}$  is located below the macrocycle polyether loop and evenly distributed on both sides of the macrocyclic cavity, indicating that the methyl group of the pyridinium can occupy the same plane as the macrocycle polyether chain and is able to swing back and forth. As a consequence of this spatial disposition, the average  $\text{C}\cdots\text{O}$  distance between the  $N$ -methyl group and the aliphatic oxygen atoms of the polyether loop ( $1.599 \pm 0.41$  Å) suggests that the interlocked structure of  $4\text{-Cl}$  is stabilised by  $\text{H}_2\text{C-H}\cdots\text{O}$  ( $\delta^+-\delta^-$ ) interactions. In contrast, for  $7\text{-Cl}$ , the carbon atom density is always out of the plane of the polyether chain due to the shorter length of the polyether loop, showing that the size of the loop (i.e., the macrocyclic cavity size) determines the binding arrangement of the interlocked structure owing to steric interactions, and ultimately has an impact on the rotaxane formation (yield) and, subsequently, its anion-binding ability.

We now focus on the anion-binding properties of the individual rotaxane systems **4** and **7** towards  $\text{Cl}^-$ ,  $\text{OAc}^-$  and  $\text{H}_2\text{PO}_4^-$  ions. The  $N_{\text{mass}}\cdots\text{X}^-$  average distance (Table 4) for

Table 4. Average distances (with standard deviations) between the anions ( $\text{X} = \text{Cl}^-$ ,  $\text{OAc}^-$  or  $\text{H}_2\text{PO}_4^{<\text{M}>-}$ ) and the centre of the binding pocket and between the hydroquinone macrocyclic rings (hyd) and pyridinium (pyr) ring axle.

Rotaxane	Distances [Å]		
	$N_{\text{mass}}\cdots\text{X}^-$	hyd $\cdots$ pyr rings	
<b>4-Cl</b>	$1.360 \pm 0.23$	$4.061 \pm 0.37$	$3.834 \pm 0.34$
<b>7-Cl</b>	$1.424 \pm 0.33$	$4.763 \pm 0.45$	$3.918 \pm 0.32$
<b>11-Cl</b>	$3.391 \pm 2.08$	$4.652 \pm 0.51$	$4.026 \pm 0.41$
<b>4-OAc</b> <sup>[a]</sup>	$1.800 \pm 0.18$	$4.037 \pm 0.36$	$3.684 \pm 0.25$
<b>7-OAc</b> <sup>[a]</sup>	$1.840 \pm 0.23$	$4.104 \pm 0.54$	$4.322 \pm 0.58$
<b>4-H<sub>2</sub>PO<sub>4</sub></b> <sup>[b]</sup>	$2.015 \pm 0.21$	$4.815 \pm 0.74$	$3.977 \pm 0.37$
<b>7-H<sub>2</sub>PO<sub>4</sub></b> <sup>[b]</sup>	$2.140 \pm 0.25$	$4.812 \pm 0.50$	$4.027 \pm 0.41$

[a] Distance measured to the centre of mass of the carbon and oxygen atoms. [b] Distance measured to the P atom. The standard deviations were calculated for  $N = 50000$ .

**4-Cl** ( $1.360$  Å) is shorter than for **4-OAc** ( $1.800$  Å) and **4-H<sub>2</sub>PO<sub>4</sub>** ( $2.015$  Å), indicating that oxoanions are more weakly bound than chloride, which is consistent with the experimental association constants (see Table 2). Furthermore, this structural parameter also shows that, in contrast to chloride, the polyatomic anions are located outside the interlocked binding pocket, as can be clearly seen in the snapshots of **4-OAc** and **4-H<sub>2</sub>PO<sub>4</sub>** represented in Figure 6.

In the case of **4-OAc**, the anion is almost outside the binding pocket, but it is still possible for the pyridinium methyl group to be found in the plane of the polyether loop, with the oxygen atoms of the carboxylate group swapping between the  $\text{N-H}$  binding sites and keeping the pseudo-tetrahedral binding arrangement. In contrast, in **4-H<sub>2</sub>PO<sub>4</sub>** the anion induces a significant distortion of the rotaxane structure, with increased exposure of the anion to the solvent



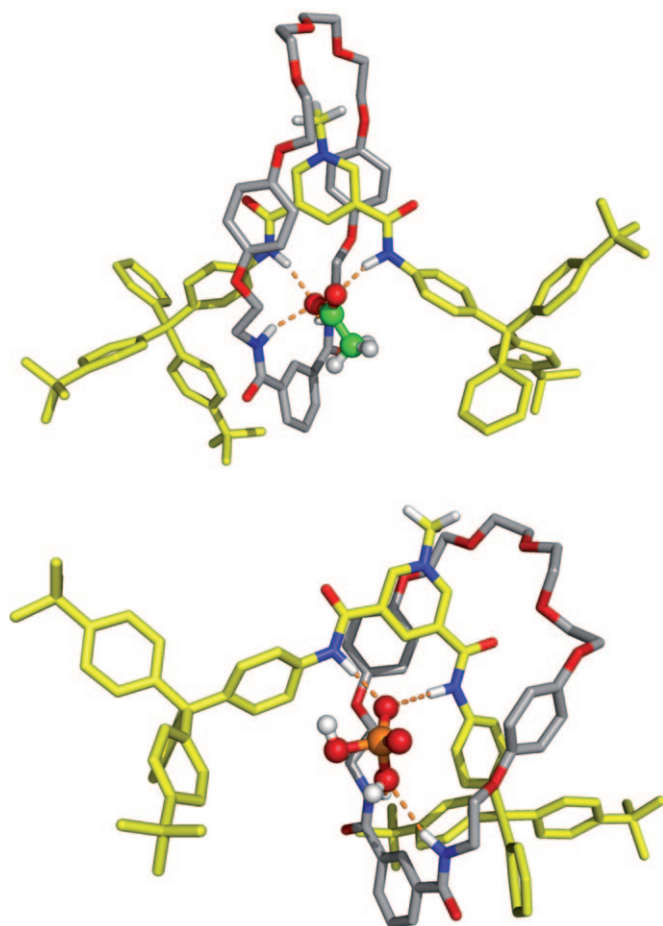


Figure 6. Snapshots of **4**-OAc (top) and **4**-H<sub>2</sub>PO<sub>4</sub> (bottom) taken at 6 ns of MD simulation. The polyatomic anions are drawn in ball and stick style. The remaining details are given in Figure 4.

medium and with the pyridinium methyl group outside the polyether chain. These distortions imply a different orientation of the axle inside the macrocycle, on binding these oxoanions, which might account for the notable upfield perturbations of the pyridinium proton ( $\gamma$ ) observed in the acetate and dihydrogen phosphate NMR titration experiments (discussed above). Figure 7 shows the different orientations observed for the pyridinium axle in representative snapshots of **4**-Cl, **4**-OAc, and **4**-H<sub>2</sub>PO<sub>4</sub>.

As one moves from Cl<sup>−</sup> to OAc<sup>−</sup> to H<sub>2</sub>PO<sub>4</sub><sup>−</sup>, the orthogonal coordination environment becomes increasingly distorted.

The number of solvent molecules of methanol, water and chloroform around the anions may also be useful for understanding the anion-binding process in rotaxanes **4**, **7** and **11**. Table 5 shows the average number of solvent molecules found within the first and

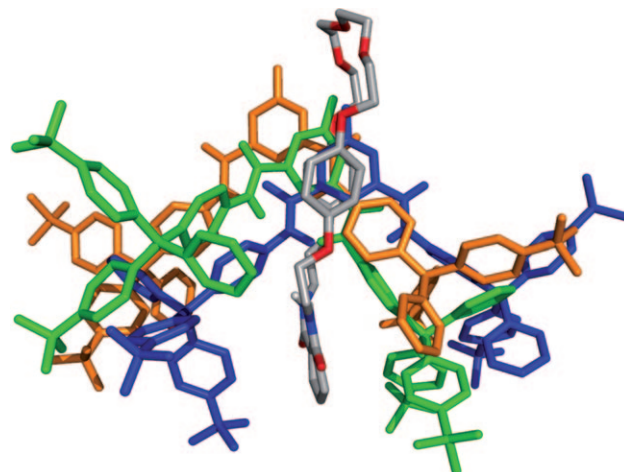


Figure 7. Superposition of the rotaxane structures **4**-Cl (blue), **4**-OAc (green) and **4**-H<sub>2</sub>PO<sub>4</sub> (orange) showing the different axle orientations.

second solvent shells of Cl<sup>−</sup>, OAc<sup>−</sup> and H<sub>2</sub>PO<sub>4</sub><sup>−</sup> during the course of the MD simulations.

For all rotaxanes, methanol preferentially solvates the anions in comparison with water, leading to a higher average number of molecules of methanol in both the first and second solvation shells. Chloroform, as expected, solvates the anions very poorly and the number of molecules of chloroform only increases significantly when one approaches the bulk. For example, the second solvation shell of OAc<sup>−</sup> bound to **4** and **7** has a significant average number of chloroform molecules, 2.1 and 2.5, respectively, which is explained by the fact that the acetate methyl group is far away from the binding pocket and the 5 Å cut-off approaches the solution bulk. Since chloroform does not interact significantly with the anions, the remaining discussion will be focused only on methanol and water molecules.

The first water and methanol solvation shell for the chloride anion increases in number of molecules in the following order **4**-Cl < **7**-Cl < **11**-Cl, meaning that chloride is increasingly more exposed to solvent molecules. The same conclusion can be drawn from the second solvation shell. The smallest chloride association constant is therefore expected to be found for rotaxane **11**, due to its labile behaviour. In contrast, the strongest association is with rotaxane **4** due to the

Table 5. Average number (maximum and minimum in parenthesis) of methanol, water and chloroform molecules closer than 3.4 Å (1st shell) and 5 Å (2nd shell) to the anion (Cl<sup>−</sup>, OAc<sup>−</sup> and H<sub>2</sub>PO<sub>4</sub><sup>−</sup>)<sup>[a]</sup> for **4**, **7** and **11**.

		Methanol		Water		Chloroform	
		1st shell	2nd shell	1st shell	2nd shell	1st shell	2nd shell
<b>4</b>	Cl <sup>−</sup>	1.5 (0–4)	3.2 (0–7)	0.7 (0–4)	1.2 (0–6)	0.0 (0–2)	0.4 (0–4)
	OAc <sup>−</sup>	1.4 (0–6)	3.1 (0–10)	0.4 (0–4)	0.9 (0–6)	0.3 (0–3)	2.1 (0–6)
	H <sub>2</sub> PO <sub>4</sub> <sup>−</sup>	2.0 (0–5)	3.2 (0–7)	0.8 (0–4)	1.2 (0–8)	0.0 (0–2)	0.8 (0–4)
<b>7</b>	Cl <sup>−</sup>	1.6 (0–4)	3.3 (0–8)	0.9 (0–7)	1.6 (0–11)	0.0 (0–1)	0.3 (0–4)
	OAc <sup>−</sup>	1.5 (0–6)	3.3 (0–9)	0.3 (0–3)	0.6 (0–5)	0.4 (0–3)	2.5 (0–7)
	H <sub>2</sub> PO <sub>4</sub> <sup>−</sup>	2.7 (0–6)	4.2 (1–9)	0.6 (0–4)	1.1 (0–6)	0.0 (0–2)	0.5 (0–4)
<b>11</b>	Cl <sup>−</sup>	1.9 (0–7)	3.7 (0–14)	1.2 (0–9)	2.2 (0–19)	0.0 (0–2)	0.2 (0–3)

[a] For OAc<sup>−</sup>, the distances are measured to the centre of mass formed by the O and C atoms. For H<sub>2</sub>PO<sub>4</sub><sup>−</sup> the distances are measured to P.

more “buried” position of  $\text{Cl}^-$  inside the binding pocket, leading to a relatively small exposure to solvent molecules.

The effect of the size of the polyether chain on the binding affinities of **4** and **7** for the polyatomic anions is also evident. As for chloride, the first and second solvation shells of the anions increases in number of molecules with decreasing chain size, suggesting that the association constants with  $\text{OAc}^-$  and  $\text{H}_2\text{PO}_4^-$  should be of larger magnitude for **4** than for **7**. This is indeed observed in the experimentally determined association constants.

## Conclusion

With the objective of highlighting the potential advantages of interlocked host systems for anion-recognition applications, a series of eight new [2]rotaxane host molecules have been prepared, including the first sulfonamide interlocked system, through a new, versatile chloride-anion-templating pathway.  $^1\text{H}$  NMR anion-titration-binding investigations demonstrate the ability of the rotaxanes’ three-dimensional binding domains to exhibit high degrees of chloride anion selectivity in competitive aqueous solvent media. The interlocked host’s chloride-anion-binding affinity can be further enhanced and tuned through the attachment of electron withdrawing substituents to the macrocycle’s isophthalamide motif and by increasing the positive charge with pyridinium group modification. In particular, the orthogonal cavity disposition of the two 3,5-bis(amide)-substituted pyridinium motifs of the dicationic rotaxane **10**·( $\text{PF}_6$ )<sub>2</sub> impressively enables this interlocked host to recognise chloride in 35% water, wherein no evidence of the binding of oxoanions, acetate or dihydrogen phosphate, is detected. The larger, basic oxoanions cannot penetrate the rotaxane’s interlocked, buried binding pocket. The combination of NMR spectroscopy, X-ray structural analysis and molecular-dynamics simulations were used to explain the rotaxane formation yields, anion-binding strengths and selectivity trends. Importantly, it is the near total encapsulation of the chloride anion guest by the respective rotaxane’s isophthalamide macrocycle and pyridinium axle binding groups that results in the efficacy of halide recognition and templation. Molecular dynamics simulation studies show that as chloride is increasingly exposed to solvent molecules, as is the case with the unfavourable conformational restrictions imposed by the sulfonamide interlocked rotaxane system, the halide anion is complexed more weakly and is a less efficient templating reagent. The design and manipulation of the unique topological cavities of mechanically bonded molecules for anion recognition and sensing applications is continuing in our laboratories.

## Experimental Section

**General considerations:** Commercially available solvents and chemicals were used without further purification unless otherwise stated. Where dry solvents were used, they were degassed with nitrogen, dried by pass-

ing through an MBraun MPSP-800 column and then used immediately. Triethylamine was distilled from and stored over potassium hydroxide. Water was deionised and microfiltered by using a Milli-Q Millipore machine.

$^1\text{H}$ ,  $^{13}\text{C}\{^1\text{H}\}$ ,  $^{19}\text{F}\{^1\text{H}\}$  and  $^{31}\text{P}\{^1\text{H}\}$  NMR spectra were recorded on Varian Mercury-VX 300 and Bruker AVI500 spectrometers. Mass spectrometry was carried out on a Bruker micrOTOF spectrometer. All new rotaxanes were characterised by  $^1\text{H}$  and  $^{13}\text{C}\{^1\text{H}\}$  NMR spectroscopy and ESMS.

Axles **1**-Cl and **1**-PF<sub>6</sub>,<sup>[13a]</sup> bis(amine) **2**,<sup>[16]</sup> and rotaxanes **5**-Cl and **5**-PF<sub>6</sub>,<sup>[14]</sup> were prepared according to reported procedures. The synthesis of bis(amine) **3** is given in the Supporting Information.

### General procedure for rotaxane synthesis

**Method 1:** Axle **1**-Cl (100 mg, 0.093 mmol) and the appropriate bis(amine) (0.093 mmol) were dissolved in dry  $\text{CH}_2\text{Cl}_2$  (20 mL) and stirred under a nitrogen atmosphere for 15 min. Triethylamine (24  $\mu\text{L}$ , 0.23 mmol) was added to the reaction mixture, followed immediately by addition of the appropriate acid chloride (0.093 mmol) in dry  $\text{CH}_2\text{Cl}_2$  (5 mL). The reaction was stirred under  $\text{N}_2$  for 1 h, before washing with 10%  $\text{HCl}_{(\text{aq})}$  (2  $\times$  25 mL) and  $\text{H}_2\text{O}$  (2  $\times$  25 mL). The organic layer was dried over anhydrous  $\text{MgSO}_4$ , the solvent removed in vacuo and the resulting crude yellow solid purified by preparative TLC.

**Method 2:** Isophthalic acid (8.3 mg, 0.05 mmol) was suspended in dry  $\text{CH}_3\text{CN}$  (5 mL). This was followed by addition of *N*-hydroxysuccinamide (13.8 mg, 0.12 mmol) and then *N,N*-dicyclohexylcarbodiimide (22.7 mg, 0.11 mmol). The reaction mixture was stirred at RT for 16 h, then filtered. The filtrate was concentrated in vacuo, re-dissolved in dry  $\text{CH}_2\text{Cl}_2$  (2 mL) and added to a solution of axle **1** (0.046 mmol), bis(amine) **2** (21.5 mg, 0.046 mmol) and  $\text{Et}_3\text{N}$  (16  $\mu\text{L}$ , 0.115 mmol) in  $\text{CH}_2\text{Cl}_2$  (10 mL). The solution was stirred under a nitrogen atmosphere for 16 h, then washed with 10%  $\text{HCl}_{(\text{aq})}$  (2  $\times$  15 mL) and  $\text{H}_2\text{O}$  (2  $\times$  15 mL), dried over anhydrous  $\text{MgSO}_4$  and the solvent removed in vacuo. The resulting crude material was purified by preparative TLC (silica; 95:5  $\text{CHCl}_3/\text{MeOH}$ ) to yield the product as a yellow solid.

**General procedure for anion exchange:** The rotaxane was dissolved in  $\text{CHCl}_3$  (15 mL) and washed with  $\text{NH}_4\text{PF}_6$  solution (0.1 M; 10  $\times$  10 mL) and  $\text{H}_2\text{O}$  (2  $\times$  10 mL). The organic layer was dried over  $\text{MgSO}_4$  and the solvent removed in vacuo to give a yellow solid in quantitative yield.

**Rotaxane 4-Cl (method 1):** Bis(amine) **2** (60 mg, 0.093 mmol) and isophthaloyl dichloride (19 mg, 0.093 mmol) were used. Preparative TLC (silica; 95:5  $\text{CHCl}_3/\text{MeOH}$ ) gave a yellow solid (91 mg, 60%).

**Rotaxane 4-Cl (method 2):** Axle **1**-Cl (50 mg, 0.046 mmol) was used. Preparative TLC (silica; 95:5  $\text{CHCl}_3/\text{MeOH}$ ) gave a yellow solid (32 mg, 41%).  $^1\text{H}$  NMR (300 MHz,  $\text{CDCl}_3$ ):  $\delta$  = 10.40 (s, 2H; axle NH), 10.06 (s, 1H; pyridinium  $H^4$ ), 9.02 (s, 2H; pyridinium  $H^2$ ,  $H^6$ ), 8.91 (s, 1H; isophthalamide  $H^2$ ), 8.54 (brs, 2H; isophthalamide NH), 7.99 (d,  $^3J$  = 7.5 Hz, 2H; isophthalamide  $H^4$ ,  $H^6$ ), 7.83 (d,  $^3J$  = 8.4 Hz, 4H; ArHNH), 7.27–7.05 (m, 31H; ArH, isophthalamide  $H^2$ ), 6.44 (d,  $^3J$  = 8.6 Hz, 4H; hydroquinone ArH), 6.16 (d,  $^3J$  = 8.6 Hz, 4H; hydroquinone ArH), 4.66 (s, 3H;  $\text{N}^+\text{CH}_3$ ), 4.11 (t,  $^3J$  = 4.5 Hz, 4H;  $-\text{CH}_2-$ ), 3.74–3.71 (m, 20H;  $-\text{CH}_2-$ ), 1.33 ppm (s, 36H; *t*Bu);  $^{13}\text{C}\{^1\text{H}\}$  NMR (75.5 MHz,  $\text{CDCl}_3$ ):  $\delta$  = 167.0, 158.2, 153.7, 151.7, 148.3, 146.9, 145.3, 144.5, 143.5, 134.8, 133.6, 133.4, 131.7, 131.5, 131.0, 130.6, 128.5, 127.3, 125.7, 124.9, 124.2, 120.2, 114.7, 114.6, 70.7, 70.5, 70.0, 68.2, 65.6, 63.8, 49.6, 40.7, 34.3, 31.3 ppm; HRMS (ESI):  $m/z$ : calcd for  $\text{C}_{106}\text{H}_{116}\text{N}_5\text{O}_{11}$ : 1635.8699; found: 1635.8654 [ $M-\text{Cl}$ ] $^+$ .

**Rotaxane 4-PF<sub>6</sub> (general procedure for anion exchange):** By using rotaxane **4**-Cl (75 mg, 0.045 mmol) to give **4**-PF<sub>6</sub> as a yellow solid (80 mg, 100%).

**Rotaxane 4-PF<sub>6</sub> (method 2):** Axle **1**-PF<sub>6</sub> (55 mg, 0.046 mmol) was used. Preparative TLC ( $\text{SiO}_2$ ; 95:5  $\text{CHCl}_3/\text{MeOH}$ ) gave a yellow solid (15 mg, 20%).  $^1\text{H}$  NMR (300 MHz,  $\text{CDCl}_3$ ):  $\delta$  = 9.26 (s, 2H; axle NH), 8.78 (s, 2H; pyridinium  $H^2$ ,  $H^6$ ), 8.66 (s, 1H; pyridinium  $H^4$ ), 8.22 (s, 1H; isophthalamide  $H^2$ ), 8.09 (d,  $^3J$  = 7.6 Hz, 2H; isophthalamide  $H^4$ ,  $H^6$ ), 7.62 (d,  $^3J$  = 8.4 Hz, 4H; ArHNH), 7.44 (t,  $^3J$  = 7.3 Hz, 1H; isophthalamide  $H^2$ ), 7.26–7.07 (m, 32H; ArH, isophthalamide NH), 6.57 (d,  $^3J$  = 8.9 Hz, 4H; hydroquinone ArH), 6.34 (d,  $^3J$  = 8.9 Hz, 4H; hydroquinone ArH), 4.26 (s, 3H;  $\text{N}^+\text{CH}_3$ ), 4.11 (m, 4H;  $-\text{CH}_2-$ ), 4.00–3.95 (m, 20H;  $-\text{CH}_2-$ ),

1.32 ppm (s, 36H; *t*Bu);  $^{13}\text{C}\{^1\text{H}\}$  NMR (75.5 MHz,  $\text{CDCl}_3$ ):  $\delta$  = 166.9, 158.6, 152.9, 151.7, 148.6, 146.8, 145.0, 144.4, 143.3, 134.5, 133.9, 131.9, 131.6, 131.0, 130.6, 129.0, 127.4, 125.8, 124.3, 123.5, 119.8, 115.9, 114.7, 70.6, 70.4, 70.0, 67.5, 66.9, 63.8, 49.3, 39.7, 34.3, 31.3 ppm;  $^{19}\text{F}\{^1\text{H}\}$  NMR (282.4 MHz,  $\text{CDCl}_3$ ):  $\delta$  = -70.0 ppm (d,  $^1J$  = 710 Hz,  $\text{PF}_6^-$ );  $^{31}\text{P}\{^1\text{H}\}$  NMR (121.6 MHz,  $\text{CDCl}_3$ ):  $\delta$  = -144.0 ppm (sept,  $^1J$  = 710 Hz,  $\text{PF}_6^-$ ); HRMS (ESI):  $m/z$ : calcd for  $\text{C}_{106}\text{H}_{116}\text{N}_5\text{O}_{11}$ : 1635.8699; found: 1635.8691 [ $M-\text{PF}_6$ ] $^+$ .

**Rotaxane 6-Cl (method 1):** Bis(amine) **2** (60 mg, 0.093 mmol) and 5-nitroisophthaloyl dichloride (23 mg, 0.093 mmol) were used. Preparative TLC (silica; 93:7  $\text{CHCl}_3/\text{MeOH}$ ) gave a yellow solid (87 mg, 55%).  $^1\text{H}$  NMR (300 MHz,  $\text{CDCl}_3$ ):  $\delta$  = 10.27 (s, 2H; axle NH), 10.02 (s, 1H; pyridinium  $H^4$ ), 9.37 (s, 1H; isophthalamide  $H^4$ ), 8.99 (s, 2H; isophthalamide  $H^2$ ,  $H^6$ ), 8.91 (d,  $^3J$  = 1.2 Hz, 2H; pyridinium  $H^2$ ,  $H^6$ ), 8.68 (t,  $^3J$  = 3.8 Hz, 2H; isophthalamide NH), 7.86 (d,  $^3J$  = 8.8 Hz, 4H; ArHNH), 7.26–6.99 (m, 30H; ArH), 6.47 (d,  $^3J$  = 9.1 Hz, 4H; hydroquinone ArH), 6.17 (d,  $^3J$  = 9.1 Hz, 4H; hydroquinone ArH), 4.71 (s, 3H;  $\text{N}^+\text{CH}_3$ ), 4.13 (t,  $^3J$  = 4.7 Hz, 4H;  $-\text{CH}_2-$ ), 3.77–3.72 (m, 20H;  $-\text{CH}_2-$ ), 1.32 ppm (s, 36H; *t*Bu);  $^{13}\text{C}\{^1\text{H}\}$  NMR (75.5 MHz,  $\text{CDCl}_3$ ):  $\delta$  = 158.0, 153.3, 151.8, 148.5, 146.7, 145.3, 144.8, 143.3, 137.1, 135.2, 134.7, 133.6, 131.8, 130.9, 130.5, 130.0, 127.3, 126.4, 125.8, 124.2, 120.3, 114.7, 70.7, 70.5, 70.0, 68.4, 65.4, 63.7, 49.8, 41.0, 34.3, 31.3 ppm; HRMS (ESI):  $m/z$ : calcd for  $\text{C}_{106}\text{H}_{116}\text{N}_6\text{O}_{13}$ : 1680.8556; found: 1680.8631 [ $M-\text{Cl}$ ] $^+$ .

**Rotaxane 6- $\text{PF}_6$  (general procedure for anion exchange):** By using rotaxane 6-Cl (75 mg, 0.044 mmol) to give 6- $\text{PF}_6$  as a yellow solid (80 mg, 100%).  $^1\text{H}$  NMR (300 MHz,  $\text{CDCl}_3$ ):  $\delta$  = 9.93 (brs, 2H; axle NH), 8.97 (s, 3H; pyridinium  $H^2$ ,  $H^4$ ,  $H^6$ ), 8.65 (s, 2H; isophthalamide  $H^2$ ,  $H^6$ ), 8.51 (s, 1H isophthalamide  $H^4$ ), 7.65 (d,  $^3J$  = 8.5 Hz, 4H; ArHNH), 7.28–7.07 (m, 32H; ArH, isophthalamide NH), 6.64 (d,  $^3J$  = 8.1 Hz, 4H; hydroquinone ArH), 6.35 (d,  $^3J$  = 8.1 Hz, 4H; hydroquinone ArH), 4.06–4.03 (m, 7H;  $\text{N}^+\text{CH}_3$ ,  $-\text{CH}_2-$ ), 3.75–3.70 (m, 16H;  $-\text{CH}_2-$ ), 3.57 (brs, 4H;  $-\text{CH}_2-$ ), 1.32 ppm (s, 36H; *t*Bu);  $^{13}\text{C}\{^1\text{H}\}$  NMR (75.5 MHz,  $\text{CDCl}_3$ ):  $\delta$  = 164.5, 158.8, 153.0, 151.6, 148.7, 146.7, 145.2, 144.6, 143.3, 136.1, 134.5, 134.0, 132.0, 131.0, 130.5, 127.4, 126.3, 125.9, 124.3, 119.8, 115.9, 114.7, 70.6, 70.5, 70.1, 67.3, 66.7, 63.8, 49.4, 39.9, 34.3, 31.3 ppm;  $^{19}\text{F}\{^1\text{H}\}$  NMR (282.4 MHz,  $\text{CDCl}_3$ ):  $\delta$  = -70.0 ppm (d,  $^1J$  = 713 Hz,  $\text{PF}_6^-$ );  $^{31}\text{P}\{^1\text{H}\}$  NMR (121.6 MHz,  $\text{CDCl}_3$ ):  $\delta$  = -144.0 ppm (sept,  $^1J$  = 713 Hz,  $\text{PF}_6^-$ ); HRMS (ESI):  $m/z$ : calcd for  $\text{C}_{106}\text{H}_{116}\text{N}_6\text{O}_{13}$ : 1680.8556; found: 1680.8534 [ $M-\text{PF}_6$ ] $^+$ .

**Rotaxane 7-Cl (method 1):** Bis(amine) **3** (46 mg, 0.093 mmol) and isophthaloyl dichloride (19 mg, 0.093 mmol) were used. Preparative TLC (silica; 9:1  $\text{CHCl}_3/\text{MeOH}$ ) gave a yellow solid (62 mg, 42%).  $^1\text{H}$  NMR (300 MHz, 1:1  $\text{CDCl}_3/\text{CD}_3\text{OD}$ ):  $\delta$  = 9.58 (s, 1H; pyridinium  $H^4$ ), 9.46 (s, 2H; pyridinium  $H^2$ ,  $H^6$ ), 8.80 (t,  $^4J$  = 1.5 Hz, 1H; isophthalamide  $H^2$ ), 7.95 (dd,  $^3J$  = 7.9,  $^4J$  = 1.5 Hz, 2H; isophthalamide  $H^4$ ,  $H^6$ ), 7.68 (d,  $^3J$  = 8.7 Hz, 4H; ArHNH), 7.25–7.05 (m, 31H; ArH, isophthalamide  $H^2$ ), 6.38 (d,  $^3J$  = 9.0 Hz, 4H; hydroquinone ArH), 6.11 (d,  $^3J$  = 9.0 Hz, 4H; hydroquinone ArH), 4.44 (s, 3H;  $\text{N}^+\text{CH}_3$ ), 4.08 (t,  $^3J$  = 4.7 Hz, 4H;  $-\text{CH}_2-$ ), 3.88–3.85 (m, 12H;  $-\text{CH}_2-$ ), 3.67 (t,  $^3J$  = 4.7 Hz, 4H;  $-\text{CH}_2-$ ), 1.29 ppm (s, 36H; *t*Bu);  $^{13}\text{C}\{^1\text{H}\}$  NMR (75.5 MHz, 1:1  $\text{CDCl}_3/\text{CD}_3\text{OD}$ ):  $\delta$  = 168.9, 159.5, 153.7, 152.5, 149.3, 147.7, 145.5, 144.4, 139.6, 135.5, 134.2, 133.5, 132.4, 132.1, 131.7, 131.4, 129.6, 128.1, 126.5, 125.0, 121.1, 115.3, 114.7, 71.6, 70.9, 67.9, 66.3, 64.6, 41.3, 34.9, 31.8, 30.3 ppm; HRMS (ESI):  $m/z$ : calcd for  $\text{C}_{104}\text{H}_{112}\text{N}_5\text{O}_{10}$ : 1591.8443; found: 1591.7578 [ $M-\text{Cl}$ ] $^+$ .

**Rotaxane 7- $\text{PF}_6$  (general procedure for anion exchange):** By using rotaxane 7-Cl (50 mg, 0.031 mmol) to give 7- $\text{PF}_6$  as a yellow solid (53 mg, 100%).  $^1\text{H}$  NMR (300 MHz, 1:1  $\text{CDCl}_3/\text{CD}_3\text{OD}$ ):  $\delta$  = 9.91 (s, 2H; pyridinium NH), 9.27 (s, 2H; pyridinium  $H^2$ ,  $H^6$ ), 9.04 (s, 1H; pyridinium  $H^4$ ), 8.50 (s, 1H; isophthalamide  $H^2$ ), 8.10 (brs, 2H; isophthalamide NH), 7.94 (dd,  $^3J$  = 7.9,  $^4J$  = 1.6 Hz, 2H; isophthalamide  $H^4$ ,  $H^6$ ), 7.51 (d,  $^3J$  = 8.8 Hz, 4H; ArHNH), 7.39 (t,  $^3J$  = 7.9 Hz, 1H; isophthalamide  $H^2$ ), 7.26–7.06 (m, 30H; ArH), 6.43 (d,  $^3J$  = 9.1 Hz, 4H; hydroquinone ArH), 6.22 (d,  $^3J$  = 9.1 Hz, 4H; hydroquinone ArH), 4.51 (s, 3H;  $\text{N}^+\text{CH}_3$ ), 3.94 (t,  $^3J$  = 4.6 Hz, 4H;  $-\text{CH}_2-$ ), 3.88–3.87 (m, 12H;  $-\text{CH}_2-$ ), 3.59–3.54 (m, 4H;  $-\text{CH}_2-$ ), 1.29 ppm (s, 36H; *t*Bu);  $^{13}\text{C}\{^1\text{H}\}$  NMR (75.5 MHz, 1:1  $\text{CDCl}_3/\text{CD}_3\text{OD}$ ):  $\delta$  = 168.4, 159.2, 153.4, 152.2, 149.1, 147.5, 145.4, 144.1, 135.1, 134.1, 133.5, 132.3, 131.6, 131.2, 129.4, 127.9, 126.4, 125.3, 124.9, 121.5, 120.8, 115.2, 114.6, 71.3, 70.7, 67.7, 66.3, 64.4, 40.8, 34.8, 31.7 ppm;

$^{19}\text{F}\{^1\text{H}\}$  NMR (282.4 MHz 1:1  $\text{CDCl}_3/\text{CD}_3\text{OD}$ ):  $\delta$  = -74.5 ppm (d,  $^1J$  = 710 Hz,  $\text{PF}_6^-$ );  $^{31}\text{P}\{^1\text{H}\}$  NMR (121.6 MHz, 1:1  $\text{CDCl}_3/\text{CD}_3\text{OD}$ ):  $\delta$  = -143.7 ppm (sept,  $^1J$  = 710 Hz,  $\text{PF}_6^-$ ); HRMS (ESI):  $m/z$ : calcd for  $\text{C}_{104}\text{H}_{112}\text{N}_5\text{O}_{10}$ : 1591.8443; found: 1591.8391 [ $M-\text{PF}_6$ ] $^+$ .

**Rotaxane 8-Cl (method 1):** Bis(amine) **3** (46 mg, 0.093 mmol) and 3,5-pyridine dicarbonyl dichloride (16 mg, 0.093 mmol) were used. Preparative TLC (silica; 9:1  $\text{CHCl}_3/\text{MeOH}$ ) gave a yellow solid (55 mg, 36%).  $^1\text{H}$  NMR (300 MHz, 1:1  $\text{CDCl}_3/\text{CD}_3\text{OD}$ ):  $\delta$  = 9.58 (s, 1H; pyridinium  $H^4$ ), 9.51 (s, 2H; pyridinium  $H^2$  &  $H^6$ ), 9.25 (t,  $^4J$  = 2.1 Hz, 1H; pyridine  $H^4$ ), 9.09 (d,  $^4J$  = 2.1 Hz, 2H; pyridine  $H^2$ ,  $H^6$ ), 7.68 (d,  $^3J$  = 8.8 Hz, 4H; HNArH), 7.26–7.03 (m, 30H; ArH), 6.42 (d,  $^3J$  = 9.1 Hz, 4H; hydroquinone ArH), 6.13 (d,  $^3J$  = 9.1 Hz, 4H; hydroquinone ArH), 4.56 (s, 3H;  $\text{N}^+\text{CH}_3$ ), 4.06 (t,  $^3J$  = 4.6 Hz, 4H;  $-\text{CH}_2-$ ), 3.90–3.86 (m, 12H;  $-\text{CH}_2-$ ), 3.66 (t,  $^3J$  = 4.6 Hz, 4H;  $-\text{CH}_2-$ ), 1.29 ppm (s, 36H; *t*Bu);  $^{13}\text{C}\{^1\text{H}\}$  NMR (75.5 MHz, 1:1  $\text{CDCl}_3/\text{CD}_3\text{OD}$ ):  $\delta$  = 166.5, 159.8, 153.7, 152.8, 152.6, 149.5, 147.8, 145.9, 144.5, 139.0, 135.5, 134.8, 133.6, 132.6, 131.8, 131.5, 129.4, 128.3, 126.7, 125.2, 121.6, 115.5, 114.8, 71.7, 71.0, 68.1, 66.4, 64.8, 41.6, 35.0, 31.9, 30.5 ppm; HRMS (ESI):  $m/z$ : calcd for  $\text{C}_{103}\text{H}_{111}\text{N}_6\text{O}_{10}$ : 1592.8395; found: 1592.7850 [ $M-\text{Cl}$ ] $^+$ .

**Rotaxane 8- $\text{PF}_6$  (general procedure for anion exchange):** By using rotaxane 8-Cl (50 mg, 0.031 mmol) to give 8- $\text{PF}_6$  as a yellow solid (53 mg, 100%).  $^1\text{H}$  NMR (300 MHz, 1:1  $\text{CDCl}_3/\text{CD}_3\text{OD}$ ):  $\delta$  = 9.36 (s, 2H; pyridinium  $H^2$ ,  $H^6$ ), 9.10 (d,  $^4J$  = 2.1 Hz, 2H; pyridine  $H^2$ ,  $H^6$ ), 9.06 (s, 1H; pyridinium  $H^4$ ), 9.00 (t,  $^4J$  = 2.1 Hz, 1H; pyridine  $H^4$ ), 7.55 (d,  $^3J$  = 8.8 Hz, 4H; HNArH), 7.26–7.06 (m, 30H; ArH), 6.43 (d,  $^3J$  = 9.1 Hz, 4H; hydroquinone ArH), 6.22 (d,  $^3J$  = 9.1 Hz, 4H; hydroquinone ArH), 4.58 (s, 3H;  $\text{N}^+\text{CH}_3$ ), 3.94 (brs, 4H;  $-\text{CH}_2-$ ), 3.89–3.87 (m, 12H;  $-\text{CH}_2-$ ), 3.55 (brs, 4H;  $-\text{CH}_2-$ ), 1.29 ppm (s, 36H; *t*Bu);  $^{13}\text{C}\{^1\text{H}\}$  NMR (75.5 MHz, 1:1  $\text{CDCl}_3/\text{CD}_3\text{OD}$ ):  $\delta$  = 166.4, 159.5, 153.43, 152.4, 151.8, 149.4, 147.7, 147.4, 146.1, 144.3, 141.1, 135.2, 133.7, 132.6, 131.7, 131.4, 130.1, 128.2, 126.7, 125.1, 121.4, 115.6, 114.8, 71.4, 70.9, 68.0, 66.7, 64.7, 40.4, 35.0, 31.8 ppm;  $^{19}\text{F}\{^1\text{H}\}$  NMR (282.4 MHz, 1:1  $\text{CDCl}_3/\text{CD}_3\text{OD}$ ):  $\delta$  = -73.0 ppm (d,  $^1J$  = 712 Hz,  $\text{PF}_6^-$ );  $^{31}\text{P}\{^1\text{H}\}$  NMR (121.6 MHz, 1:1  $\text{CDCl}_3/\text{CD}_3\text{OD}$ ):  $\delta$  = -144.2 ppm (sept,  $^1J$  = 712 Hz,  $\text{PF}_6^-$ ); HRMS (ESI):  $m/z$ : calcd for  $\text{C}_{103}\text{H}_{111}\text{N}_6\text{O}_{10}$ : 1592.8395; found: 1592.8319 [ $M-\text{PF}_6$ ] $^+$ .

**Rotaxane 9-Cl (method 1):** Bis(amine) **3** (46 mg, 0.093 mmol) and 5-nitroisophthaloyl dichloride (23 mg, 0.093 mmol) were used. Preparative TLC (silica; 93:7  $\text{CHCl}_3/\text{MeOH}$ ) gave a yellow solid (64 mg, 41%).  $^1\text{H}$  NMR (300 MHz, 1:1  $\text{CDCl}_3/\text{CD}_3\text{OD}$ ):  $\delta$  = 9.62 (s, 1H; pyridinium  $H^4$ ), 9.52 (s, 2H; pyridinium  $H^2$ ,  $H^6$ ), 9.30 (brt,  $^4J$  = 1.4 Hz, 1H; isophthalamide  $H^2$ ), 8.84 (d,  $^4J$  = 1.4 Hz, 2H; isophthalamide  $H^4$ ,  $H^6$ ), 7.72 (d,  $^3J$  = 8.7 Hz, 4H; HNArH), 7.25–6.99 (m, 30H; ArH), 6.42 (d,  $^3J$  = 9.1 Hz, 4H; hydroquinone ArH), 6.13 (d,  $^3J$  = 9.1 Hz, 4H; hydroquinone ArH), 4.58 (s, 3H;  $\text{N}^+\text{CH}_3$ ), 4.10 (t,  $^3J$  = 4.4 Hz, 4H;  $-\text{CH}_2-$ ), 3.89–3.84 (m, 12H;  $-\text{CH}_2-$ ), 3.69 (t,  $^3J$  = 4.4 Hz, 4H;  $-\text{CH}_2-$ ) 1.30 ppm (s, 36H; *t*Bu);  $^{13}\text{C}\{^1\text{H}\}$  NMR (75.5 MHz, 1:1  $\text{CDCl}_3/\text{CD}_3\text{OD}$ ):  $\delta$  = 165.7, 159.4, 153.6, 152.6, 149.3, 149.2, 147.5, 144.1, 135.8, 135.2, 133.4, 132.4, 131.6, 131.2, 128.0, 126.9, 126.5, 124.9, 121.2, 115.3, 114.6, 71.5, 70.9, 67.9, 66.1, 64.5, 41.8, 34.9, 31.8, 30.3 ppm; HRMS (ESI):  $m/z$ : calcd for  $\text{C}_{106}\text{H}_{114}\text{N}_7\text{O}_{12}$ : 1636.8394; found: 1636.7740 [ $M-\text{Cl}$ ] $^+$ .

**Rotaxane 9- $\text{PF}_6$  (general procedure for anion exchange):** By using rotaxane 9-Cl (50 mg, 0.030 mmol) to give 9- $\text{PF}_6$  as a yellow solid (53 mg, 100%).  $^1\text{H}$  NMR (300 MHz, 1:1  $\text{CDCl}_3/\text{CD}_3\text{OD}$ ):  $\delta$  = 9.41 (s, 2H; pyridinium  $H^2$ ,  $H^6$ ), 9.15 (s, 1H; pyridinium  $H^4$ ), 9.06 (s, 1H; isophthalamide  $H^2$ ), 8.84 (s, 2H; isophthalamide  $H^4$ ,  $H^6$ ), 7.57 (d,  $^3J$  = 8.8 Hz, 4H; HNArH), 7.25–7.03 (m, 30H; ArH), 6.43 (d,  $^3J$  = 8.4 Hz, 4H; hydroquinone ArH), 3.97–3.58 (d,  $^3J$  = 8.4 Hz, 4H; hydroquinone ArH), 4.59 (s, 3H;  $\text{N}^+\text{CH}_3$ ), 3.97 (brs, 4H;  $-\text{CH}_2-$ ), 3.89–3.87 (m, 12H;  $-\text{CH}_2-$ ), 3.58 (brs, 4H;  $-\text{CH}_2-$ ), 1.30 ppm (s, 36H; *t*Bu);  $^{13}\text{C}\{^1\text{H}\}$  NMR (125 MHz, 1:1  $\text{CDCl}_3/\text{CD}_3\text{OD}$ ):  $\delta$  = 165.5, 159.2, 153.5, 152.4, 149.1, 147.4, 145.4, 144.0, 135.7, 135.1, 133.3, 132.2, 131.5, 131.1, 129.0, 127.9, 126.8, 126.3, 124.8, 121.0, 115.2, 114.4, 71.4, 70.7, 69.7, 66.0, 64.3, 53.5, 41.7, 34.7, 31.7 ppm;  $^{19}\text{F}\{^1\text{H}\}$  NMR (282.4 MHz, 1:1  $\text{CDCl}_3/\text{CD}_3\text{OD}$ ):  $\delta$  = -73.0 ppm (d,  $^1J$  = 712 Hz,  $\text{PF}_6^-$ );  $^{31}\text{P}\{^1\text{H}\}$  NMR (121.6 MHz, 1:1  $\text{CDCl}_3/\text{CD}_3\text{OD}$ ):  $\delta$  = -144.0 ppm (sept,  $^1J$  = 712 Hz,  $\text{PF}_6^-$ ); HRMS (ESI):  $m/z$ : calcd for  $\text{C}_{106}\text{H}_{114}\text{N}_7\text{O}_{12}$ : 1636.8394; found: 1636.8242 [ $M-\text{PF}_6$ ] $^+$ .

**Rotaxane 10-( $\text{PF}_6$ ) $_2$ :** Rotaxane 8- $\text{PF}_6$  (50 mg, 0.030 mmol) was dissolved in MeI (5 mL) and the solution was heated at reflux under a nitrogen at-



mosphere for 16 h. The solvent was removed in vacuo, and the yellow residue re-dissolved in  $\text{CHCl}_3$  and washed with  $\text{NH}_4\text{PF}_6(\text{aq})$  (0.1 M; 10 × 10 mL) and  $\text{H}_2\text{O}$  (2 × 10 mL). The organic layer was dried over  $\text{MgSO}_4$  and the solvent removed in vacuo to give a yellow solid (51 mg, 95%).  $^1\text{H}$  NMR (500 MHz, 1:1  $\text{CDCl}_3/\text{CD}_3\text{OD}$ ):  $\delta$  = 9.42 (s, 1H; axle pyridinium  $\text{H}^4$ ), 9.39 (s, 2H; axle pyridinium  $\text{H}^2$ ,  $\text{H}^6$ ), 9.19 (s, 1H; macrocycle pyridinium  $\text{H}^4$ ), 8.68 (d,  $^3J$  = 8.8 Hz, 4H;  $\text{HNArH}$ ), 7.32–7.11 (m, 34H; stopper  $\text{ArH}$ ), 6.65 (d,  $^3J$  = 8.8 Hz, 4H; hydroquinone  $\text{ArH}$ ), 6.33 (d,  $^3J$  = 8.8 Hz, 4H; hydroquinone  $\text{ArH}$ ), 4.48 (s, 3H; axle  $\text{N}^+\text{CH}_3$ ), 4.04 (t,  $^3J$  = 4.9 Hz, 4H;  $-\text{CH}_2-$ ), 3.93 (s, 3H; macrocycle  $\text{N}^+\text{CH}_3$ ), 3.76 (t,  $^3J$  = 4.5 Hz, 4H;  $-\text{CH}_2-$ ), 3.74–3.71 (m, 8H;  $-\text{CH}_2-$ ), 3.68–3.67 (m, 4H;  $-\text{CH}_2-$ ), 1.28 ppm (s, 36H;  $t\text{Bu}$ );  $^{13}\text{C}$  NMR (75.5 MHz,  $\text{CDCl}_3$ ):  $\delta$  = 160.6, 158.5, 153.0, 151.8, 148.5, 147.0, 145.3, 144.2, 143.6, 135.4, 134.6, 133.8, 131.7, 131.1, 130.7, 127.3, 125.8, 124.2, 120.0, 115.4, 114.6, 70.6, 69.8, 67.5, 66.5, 63.8, 54.8, 49.7, 49.5, 40.3, 34.3, 31.4 ppm;  $^{19}\text{F}$  NMR (282.4 MHz,  $\text{CDCl}_3$ ):  $\delta$  = −70.9 ppm (d,  $^1J$  = 710 Hz,  $\text{PF}_6^-$ );  $^{31}\text{P}$  NMR (121.6 MHz,  $\text{CDCl}_3$ ):  $\delta$  = −144.1 ppm (sept,  $^1J$  = 710 Hz,  $\text{PF}_6^-$ ); HRMS (ESI):  $m/z$ : calcd for  $\text{C}_{106}\text{H}_{117}\text{N}_6\text{O}_{11}$ : 1650.8814; found: 1650.9064 [ $\text{M}-\text{PF}_6-\text{H}$ ] $^+$ .

**Rotaxane 11-Cl (method 1):** Bis(amine) **3** (46 mg, 0.093 mmol) and 1,3-benzenedisulfonyl chloride (27 mg, 0.093 mmol) were used. Preparative TLC (silica; 93:7  $\text{CHCl}_3/\text{MeOH}$ ) gave a yellow solid (36 mg, 23%).  $^1\text{H}$  NMR (300 MHz, 1:1  $\text{CDCl}_3/\text{CD}_3\text{OD}$ ):  $\delta$  = 9.62 (s, 2H; pyridinium  $\text{H}^2$ ,  $\text{H}^6$ ), 8.89 (s, 1H; pyridinium  $\text{H}^4$ ), 8.55 (s, 1H; sulfonyl  $\text{H}^2$ ), 7.90 (d,  $^3J$  = 7.8 Hz, 2H; sulfonyl  $\text{H}^4$ ,  $\text{H}^6$ ), 7.64 (d,  $^3J$  = 8.0 Hz, 4H;  $\text{HNArH}$ ), 7.29–7.12 (m, 31H;  $\text{ArH}$ , sulfonyl  $\text{H}^2$ ), 6.41 (d,  $^3J$  = 8.4 Hz, 4H; hydroquinone  $\text{ArH}$ ), 6.20 (d,  $^3J$  = 8.4 Hz, 4H; hydroquinone  $\text{ArH}$ ), 4.57 (s, 3H;  $\text{N}^+\text{CH}_3$ ), 3.87 (brs, 4H;  $-\text{CH}_2-$ ), 3.82–3.76 (m, 12H;  $-\text{CH}_2-$ ), 3.09 (t,  $^3J$  = 4.7 Hz, 4H;  $-\text{CH}_2-$ ), 1.30 ppm (s, 36H;  $t\text{Bu}$ );  $^{13}\text{C}$  NMR (75.5 MHz, 1:1  $\text{CDCl}_3/\text{CD}_3\text{OD}$ ):  $\delta$  = 159.4, 153.2, 152.4, 149.4, 147.7, 145.5, 144.4, 142.8, 135.4, 133.3, 132.5, 131.7, 131.4, 131.0, 128.1, 126.5, 126.2, 125.0, 120.6, 116.1, 114.9, 71.4, 70.8, 67.9, 67.5, 64.6, 42.9, 34.9, 31.8, 30.3 ppm; HRMS (ESI):  $m/z$ : calcd for  $\text{C}_{102}\text{H}_{112}\text{N}_5\text{O}_{12}\text{S}_2$ : 1663.7782; found: 1663.7636 [ $\text{M}-\text{Cl}$ ] $^+$ .

**Rotaxane 11-PF<sub>6</sub> (general procedure for anion exchange):** By using rotaxane 11-Cl (30 mg, 0.018 mmol) to give 11-PF<sub>6</sub> as a yellow solid (32 mg, 100%).  $^1\text{H}$  NMR (300 MHz, 1:1  $\text{CDCl}_3/\text{CD}_3\text{OD}$ ):  $\delta$  = 9.29 (s, 2H; pyridinium  $\text{H}^2$ ,  $\text{H}^6$ ), 8.66 (s, 1H; pyridinium  $\text{H}^4$ ), 8.49 (brt,  $^4J$  = 1.7 Hz, 1H; sulfonyl  $\text{H}^2$ ), 8.01 (dd,  $^3J$  = 8.0,  $^4J$  = 1.7 Hz, 2H; sulfonyl  $\text{H}^4$ ,  $\text{H}^6$ ), 7.58 (d,  $^4J$  = 8.9 Hz, 4H;  $\text{HNArH}$ ), 7.29–7.12 (m, 31H;  $\text{ArH}$ , sulfonyl  $\text{H}^2$ ), 6.46 (d,  $^3J$  = 9.2 Hz, 4H; hydroquinone  $\text{ArH}$ ), 6.22 (d,  $^3J$  = 9.2 Hz, 4H; hydroquinone  $\text{ArH}$ ), 4.53 (s, 3H;  $\text{N}^+\text{CH}_3$ ), 3.97–3.88 (m, 16H;  $-\text{CH}_2-$ ), 3.16 (t,  $^3J$  = 5.3 Hz, 4H;  $-\text{CH}_2-$ ), 1.29 ppm (s, 36H;  $t\text{Bu}$ );  $^{13}\text{C}$  NMR (75.5 MHz, 1:1  $\text{CDCl}_3/\text{CD}_3\text{OD}$ ):  $\delta$  = 159.3, 153.2, 152.4, 149.4, 147.7, 145.8, 144.6, 143.0, 135.2, 133.8, 132.7, 131.8, 131.4, 131.1, 128.1, 126.6, 125.6, 125.1, 120.6, 116.2, 114.8, 71.2, 70.9, 67.7, 67.6, 64.6, 42.9, 34.9, 31.8, 30.3, 23.3 ppm;  $^{19}\text{F}$  NMR (282.4 MHz, 1:1  $\text{CDCl}_3/\text{CD}_3\text{OD}$ ):  $\delta$  = −72.7 ppm (d,  $^1J$  = 712 Hz,  $\text{PF}_6^-$ );  $^{31}\text{P}$  NMR (121.6 MHz, 1:1  $\text{CDCl}_3/\text{CD}_3\text{OD}$ ):  $\delta$  = −144.2 ppm (sept,  $^1J$  = 712 Hz,  $\text{PF}_6^-$ ); HRMS (ESI):  $m/z$ : calcd for  $\text{C}_{102}\text{H}_{112}\text{N}_5\text{O}_{12}\text{S}_2$ : 1663.7782; found: 1663.7624 [ $\text{M}-\text{PF}_6$ ] $^+$ .

## Acknowledgements

We thank the EPSRC for a studentship (L.M.H.) and Johnson Matthey for a CASE studentship (C.J.S.). N.L.K. acknowledges the Royal Commission for the Exhibition of 1851 for a research fellowship. P.J.C. and S.C. thank FCT for the post-doctoral grants SFRH/BPD/27082/2006 and SFRH/BPD/42357/2007, respectively. V.F. acknowledges the FCT, with co-participation of the European Community fund FEDER, for financial support under project PTDC/QUI/68582/2006. We also thank Diamond Light Source for an award of beam time on I19 (MT1880), the beamline instrument scientists for their assistance, and Dr. N. H. Rees for NMR advice.

- [1] a) A. Bianchi, K. Bowman-James, E. García-España, *Supramolecular Chemistry of Anions*, Wiley-VCH, New York **1997**; b) J. L. Sess-

- ler, P. A. Gale, W.-S. Cho, *Anion Receptor Chemistry*, RSC, Cambridge, **2006**; c) F. P. Schmidtchen, M. Berger, *Chem. Rev.* **1997**, 97, 1609–1646; d) P. D. Beer, P. A. Gale, *Angew. Chem.* **2001**, 113, 502–532; *Angew. Chem. Int. Ed.* **2001**, 40, 486–516; e) M. D. Best, S. L. Tobey, E. V. Anslyn, *Coord. Chem. Rev.* **2003**, 240, 3–15; f) J. M. Llinares, D. Powell, K. Bowman-James, *Coord. Chem. Rev.* **2003**, 240, 57–75; g) K. Choi, A. D. Hamilton, *Coord. Chem. Rev.* **2003**, 240, 101–110; h) T. J. Wedge, M. F. Hawthorne, *Coord. Chem. Rev.* **2003**, 240, 111–128; i) A. P. Davis, J.-B. Joos, *Coord. Chem. Rev.* **2003**, 240, 143–156; j) P. D. Beer, E. J. Hayes, *Coord. Chem. Rev.* **2003**, 240, 167–189; k) R. Martínez-Mañez, F. Sancenón, *Chem. Rev.* **2003**, 103, 4419–4476; l) M. H. Filby, J. W. Steed, *Coord. Chem. Rev.* **2006**, 250, 3200–3218; m) A. P. Davis, *Coord. Chem. Rev.* **2006**, 250, 2939–2951; n) E. García-España, P. Díaz, J. M. Llinares, A. Bianchi, *Coord. Chem. Rev.* **2006**, 250, 2952–2986; o) E. A. Katayev, Y. A. Ustynyuk, J. L. Sessler, *Coord. Chem. Rev.* **2006**, 250, 3004–3037; p) E. J. O’Neil, B. D. Smith, *Coord. Chem. Rev.* **2006**, 250, 3068–3080; q) R. Martínez-Mañez, F. Sancenón, *Coord. Chem. Rev.* **2006**, 250, 3081–3093; r) T. Gunnlaugsson, M. Glynn, G. M. Tocci, P. E. Kruger, F. M. Pfeffer, *Coord. Chem. Rev.* **2006**, 250, 3094–3117; s) C. R. Rice, *Coord. Chem. Rev.* **2006**, 250, 3190–3199; t) P. A. Gale, R. Quesada, *Coord. Chem. Rev.* **2006**, 250, 3219–3244; u) P. A. Gale, S. E. García-Garrido, J. Garric, *Chem. Soc. Rev.* **2008**, 37, 151–190; v) J. Pérez, L. Riera, *Chem. Soc. Rev.* **2008**, 37, 2658–2667; w) J. W. Steed, *Chem. Soc. Rev.* **2009**, 38, 506–519; x) C. Caltagirone, P. A. Gale, *Chem. Soc. Rev.* **2009**, 38, 520–563; y) S. Kubik, *Chem. Soc. Rev.* **2009**, 38, 585–605; z) Y. Hua, A. H. Flood, *Chem. Soc. Rev.* **2010**, 39, 1262–1271.
- [2] J. W. Pflugrath, F. A. Quirocho, *Nature* **1985**, 314, 257–260.
- [3] H. Luecke, F. A. Quirocho, *Nature* **1990**, 347, 402–406.
- [4] a) X. Yang, C. B. Knobler, M. F. Hawthorne, *Angew. Chem.* **1991**, 103, 1519–1521; *Angew. Chem. Int. Ed. Engl.* **1991**, 30, 1507–1508; b) Z. Zheng, C. B. Knobler, M. F. Hawthorne, *J. Am. Chem. Soc.* **1995**, 117, 5105–5113; c) J. S. Fleming, K. L. V. Mann, C.-A. Carraz, E. Psillakis, J. C. Jeffery, J. A. McCleverty, M. D. Ward, *Angew. Chem.* **1998**, 110, 1315–1318; *Angew. Chem. Int. Ed.* **1998**, 37, 1279–1281; d) R. L. Paul, Z. R. Bell, J. C. Jeffery, J. A. McCleverty, M. D. Ward, *Proc. Natl. Acad. Sci. USA* **2002**, 99, 4883–4888; e) C. S. Campos-Fernández, B. L. Schottel, H. T. Chifotides, J. K. Bera, J. Bacsá, J. M. Koomen, D. H. Russell, K. R. Dunbar, *J. Am. Chem. Soc.* **2005**, 127, 12909–12923; f) S. P. Argent, T. Riis-Johannessen, J. C. Jeffery, L. P. Harding, M. D. Ward, *Chem. Commun.* **2005**, 4647–4649.
- [5] a) R. Vilar, *Angew. Chem.* **2003**, 115, 1498–1516; *Angew. Chem. Int. Ed.* **2003**, 42, 1460–1477; b) R. Vilar, *Eur. J. Inorg. Chem.* **2008**, 357–367; c) R. Custelcean, J. Bosano, P. V. Bonnesen, V. Kertesz, B. P. Hay, *Angew. Chem.* **2009**, 121, 4085–4089; *Angew. Chem. Int. Ed.* **2009**, 48, 4025–4029.
- [6] M. Shionoya, H. Furuta, V. Lynch, A. Harriman, J. L. Sessler, *J. Am. Chem. Soc.* **1992**, 114, 5714–5722.
- [7] a) E. A. Katayev, G. Dan Pantos, M. D. Reshetova, V. N. Khrustalev, V. Lynch, Y. A. Ustynyuk, J. L. Sessler, *Angew. Chem.* **2005**, 117, 7552–7556; *Angew. Chem. Int. Ed.* **2005**, 44, 7386–7390; b) E. A. Katayev, N. V. Boev, V. N. Khrustalev, Y. A. Ustynyuk, I. G. Tananaev, J. L. Sessler, *J. Org. Chem.* **2007**, 72, 2886–2896.
- [8] D. Meshcheryakov, V. Böhmer, M. Bolte, V. Hubscher-Bruder, F. Arnaud-Neu, H. Herschbach, A. Van Dorsselaer, I. Thondorf, W. Mögelin, *Angew. Chem.* **2006**, 118, 1679–1682; *Angew. Chem. Int. Ed.* **2006**, 45, 1648–1652.
- [9] a) M. Bru, I. Alfonso, M. I. Burguete, S. V. Luis, *Angew. Chem.* **2006**, 118, 6301–6305; *Angew. Chem. Int. Ed.* **2006**, 45, 6155–6159; b) I. Alfonso, M. Bolte, M. Bru, M. I. Burguete, S. V. Luis, J. Rubio, *J. Am. Chem. Soc.* **2008**, 130, 6137–6144.
- [10] a) *Molecular Catenanes, Rotaxanes and Knots: A Journey Through the World of Molecular Topology* (Eds.: C. Dietrich-Buchecker, J.-P. Sauvage), Wiley-VCH, Weinheim, **1999**; b) V. Balzani, M. Venturi, A. Credi, *Molecular Devices and Machines—A Journey into the Nanoworld*, Wiley-VCH, Weinheim, **2003**; c) E. R. Kay, D. A. Leigh, F. Zerbetto, *Angew. Chem.* **2007**, 119, 72–196; *Angew. Chem. Int.*

- Ed.* **2007**, 46, 72–191; d) S. Saha, J. F. Stoddart, *Chem. Soc. Rev.* **2007**, 36, 77–92; e) S. J. Loeb, *Chem. Soc. Rev.* **2007**, 36, 226–235; f) B. Champin, P. Mobian, J.-P. Sauvage, *Chem. Soc. Rev.* **2007**, 36, 358–366; g) J. F. Stoddart, H. M. Colquhoun, *Tetrahedron* **2008**, 64, 8231–8263.
- [11] M. J. Chmielewski, J. J. Davis, P. D. Beer, *Org. Biomol. Chem.* **2009**, 7, 415–424.
- [12] J. J. Gassensmith, S. Matthys, J.-J. Lee, A. Wojcik, P. V. Kamat, B. D. Smith, *Chem. Eur. J.* **2010**, 16, 2916–2921.
- [13] a) J. A. Wisner, P. D. Beer, M. G. B. Drew, M. R. Sambrook, *J. Am. Chem. Soc.* **2002**, 124, 12469–12476; b) M. R. Sambrook, P. D. Beer, J. A. Wisner, R. L. Paul, A. R. Cowley, *J. Am. Chem. Soc.* **2004**, 126, 15364–15365; c) K.-Y. Ng, A. R. Cowley, P. D. Beer, *Chem. Commun.* **2006**, 3676; d) M. R. Sambrook, P. D. Beer, M. D. Lankshear, R. F. Ludlow, J. A. Wisner, *Org. Biomol. Chem.* **2006**, 4, 1529–1538; e) M. D. Lankshear, P. D. Beer, *Acc. Chem. Res.* **2007**, 40, 657–668; f) M. D. Lankshear, N. H. Evans, S. R. Bayly, P. D. Beer, *Chem. Eur. J.* **2007**, 13, 3861; g) M. S. Vickers, P. D. Beer, *Chem. Soc. Rev.* **2007**, 36, 211–225; h) B. Huang, S. M. Santos, V. Félix, P. D. Beer, *Chem. Commun.* **2008**, 4610–4612; i) K. M. Mullen, J. Mercurio, C. J. Serpell, P. D. Beer, *Angew. Chem.* **2009**, 121, 4875–4878; *Angew. Chem. Int. Ed.* **2009**, 48, 4781–4784; j) D. E. Phipps, P. D. Beer, *Tetrahedron Lett.* **2009**, 50, 3454–3457.
- [14] L. M. Hancock, P. D. Beer, *Chem. Eur. J.* **2009**, 15, 42–44.
- [15] For examples of chloride recognition in aqueous media, see: a) W. Goodall, J. A. G. Williams, *J. Chem. Soc. Dalton Trans.* **2000**, 2893–2895; b) V. Amendola, E. Bastianello, L. Fabbri, C. Mangano, P. Pallavicini, A. Perotti, A. M. Lanfredi, F. Uguzzoli, *Angew. Chem.* **2000**, 112, 3039–3042; *Angew. Chem. Int. Ed.* **2000**, 39, 2917–2920; c) D. K. Smith, *Org. Biomol. Chem.* **2003**, 1, 3874–3877; d) R. Nishiyabu, M. A. Palacios, W. Dehaen, P. Anzenbacher, Jr., *J. Am. Chem. Soc.* **2006**, 128, 11496–11504; e) X. C. Jiang, A. B. Yu, *Langmuir* **2008**, 24, 4300–4309; f) D.-W. Yoon, D. E. Groos, V. M. Lynch, C.-H. Lee, P. C. Bennett, J. L. Sessler, *Chem. Commun.* **2009**, 1109–1111.
- [16] K.-Y. Ng, V. Félix, S. M. Santos, N. H. Rees, *Chem. Commun.* **2008**, 1281–1283.
- [17] a) U. Eisner, J. Kuthan, *Chem. Rev.* **1972**, 72, 1–42; b) D. M. Stout, A. I. Meyers, *Chem. Rev.* **1982**, 82, 223–243.
- [18] J. A. Wisner, P. D. Beer, M. G. B. Drew, *Angew. Chem.* **2001**, 113, 3718–3721; *Angew. Chem. Int. Ed.* **2001**, 40, 3606–3609.
- [19] To replicate the original reaction conditions, the acid chloride condensation was carried out in the presence of AgPF<sub>6</sub> (2 equiv) to precipitate the chloride generated during the condensation reaction. The yield of this reaction was observed to be approximately 15%, only a quarter of that in which the chloride anion was present. This is another positive indication that the yield of the reaction is highly dependant on the presence of the chloride anion.
- [20] Although co-crystallised solvent was present, it could not be resolved structurally in either case and was modelled as a diffuse cloud of electrons. However, its presence and effect on the overall conformation of both of these structures, along with packing considerations, cannot be ignored, especially when compared with the molecular dynamics solution structures. Conclusions concerning the electronic effect of the nitro group are difficult to make due to the multiplicity of variables (polyether chain length and crystallisation requirements).
- [21] M. J. Hynes, *J. Chem. Soc. Dalton Trans.* **1993**, 311–312.
- [22] Anion binding investigations with axle **1**·PF<sub>6</sub> in 45:45:10 CDCl<sub>3</sub>/CD<sub>3</sub>OD/D<sub>2</sub>O revealed, as expected, very weak binding of Cl<sup>−</sup>.
- [23] D. A. Case, AMBER 10, University of California, San Francisco, **2008**.
- [24] J. Wang, R. M. Wolf, J. W. Caldwell, P. A. Kollman, D. A. Case, *J. Comput. Chem.* **2004**, 25, 1157–1174.

Received: July 21, 2010

Published online: October 28, 2010